MCB
Journals.ASM.org

WASH Knockout T Cells Demonstrate Defective Receptor Trafficking, Proliferation, and Effector Function

Joshua T. Piotrowski,[a] Timothy S. Gomez,[a,b] Renee A. Schoon,[a,b] Ashutosh K. Mangalam,[a] Daniel D. Billadeau[a,b]

Department of Immunology[a] and Division of Oncology Research and Schulze Center for Novel Therapeutics,[b] College of Medicine, Mayo Clinic, Rochester, Minnesota, USA

WASH is an Arp2/3 activator of the Wiskott-Aldrich syndrome protein superfamily that functions during endosomal trafficking processes in collaboration with the retromer and sorting nexins, but its *in vivo* function has not been examined. To elucidate the physiological role of WASH in T cells, we generated a WASH conditional knockout (WASHout) mouse model. Using $CD4^{Cre}$ deletion, we found that thymocyte development and naive T cell activation are unaltered in the absence of WASH. Surprisingly, despite normal T cell receptor (TCR) signaling and interleukin-2 production, WASHout T cells demonstrate significantly reduced proliferative potential and fail to effectively induce experimental autoimmune encephalomyelitis. Interestingly, after activation, WASHout T cells fail to maintain surface levels of TCR, CD28, and LFA-1. Moreover, the levels of the glucose transporter, GLUT1, are also reduced compared to wild-type T cells. We further demonstrate that the loss of surface expression of these receptors in WASHout cells results from aberrant accumulation within the collapsed endosomal compartment, ultimately leading to degradation within the lysosome. Subsequently, activated WASHout T cells experience reduced glucose uptake and metabolic output. Thus, we found that WASH is a newly recognized regulator of TCR, CD28, LFA-1, and GLUT1 endosome-to-membrane recycling. Aberrant trafficking of these key T cell proteins may potentially lead to attenuated proliferation and effector function.

Filamentous-actin (F-actin) polymerization at the immunological synapse (IS) is a hallmark of T cell activation and is required for optimal T cell signaling and effector functions (1). The Wiskott-Aldrich syndrome protein (WASP) superfamily of nucleation-promoting factors (NPFs), which activate the actin-related protein 2/3 (Arp2/3) complex, are important regulators of branched F-actin nucleation (2, 3). WASP, N-WASP, and the WAVE isoforms (WAVE1 to WAVE3) have been the focus of much attention over the past decade. As a result, it is well established that both WAVE2 and WASP participate in Arp2/3-dependent F-actin generation at the IS leading to the development of the F-actin-rich lamellae (4), integrin-mediated adhesion (5), receptor internalization, efficient T cell receptor (TCR) signaling, and T cell activation (6–9). However, our understanding of the contribution of NPFs to cell biology is rapidly expanding with the addition of newly recognized WASP family members, including WHAMM, which regulates endoplasmic reticulum-to-Golgi trafficking, and JMY, which not only regulates F-actin generation at the lamellae but also functions during p53-dependent gene transcription (10–12).

Recently, another highly conserved WASP family member, WASH (Wiskott-Aldrich syndrome protein and SCAR homolog) was identified (13). WASH exists in a multiprotein complex termed the SHRC (WASH regulatory complex), which is comprised of FAM21, SWIP, strumpellin, and CCDC53 (14–16). Interestingly, the SHRC is structurally analogous to the WAVE regulatory complex and is important for SHRC component stabilization and regulation of WASH activity toward Arp2/3 (15, 16). However, in contrast to the WASP and WAVE proteins, which primarily localize to the plasma membrane, mammalian WASH localizes to distinct subdomains on endomembranes, where it participates in vesicle trafficking through localized Arp2/3-dependent F-actin nucleation (14, 15). Endosomal localization of the SHRC is mediated by an interaction of the FAM21 C terminus with VPS35, a component of the retromer complex (17, 18). Using RNA interference-mediated suppression, several recent studies have identified WASH as a unique regulator of receptor trafficking at endomembranes. Specifically, WASH has been implicated in transferrin receptor (TfnR) and α5β1 integrin recycling (14, 19), as well as retromer-dependent recycling of the cation-independent mannose-6-phosphate receptor (15) and β_2 adrenergic receptor (β2AR) (20). Taken together, these studies identify WASH as a regulator of multiple receptor trafficking systems. However, the biological implications of WASH regulation remain to be established in an *in vivo* biological model.

To determine the physiologic function of WASH *in vivo*, we generated conditional *WASH* knockout (WASHout) mice. Since the WASP superfamily members WASP and WAVE have previously been demonstrated to regulate various aspects of T cell activation (2, 21), we investigated the role of WASH in T cell function. Using cre-recombinase models for T cell-specific gene excision, we found that peripheral WASHout T cells exhibited no defect in naive TCR signaling or T cell activation. However, WASHout T cells did not proliferate effectively, and mice with WASH-deficient T cells experienced reduced disease burden in experimental autoimmune encephalomyelitis (EAE). We further show that TCR, CD28, LFA-1, and GLUT1 are inefficiently trafficked after T cell activation in WASHout T cells, which ultimately led to the lysosomal degradation of these important receptors and transporter. Thus, it appears that WASH regulates the trafficking of several key proteins responsible for normal T cell effector function. Together, these results identify an important and unique physiological role for WASH in proper T cell function and provide

Received 21 September 2012 Returned for modification 15 October 2012
Accepted 20 December 2012
Published ahead of print 28 December 2012
Address correspondence to Daniel D. Billadeau, billadeau.daniel@mayo.edu.

doi:10.1128/MCB.01288-12

validation of a novel mouse model that can be further utilized to increase our understanding of WASH-dependent trafficking in a variety of biologically important systems.

MATERIALS AND METHODS

Generation of *WASH* conditional knockout mice. Conditional *WASH* knockout mice were generated in collaboration with the Transgenic and Gene Targeted Mouse Shared Resource at the Mayo Clinic according to established protocols (22). The *WASH* knockout targeting construct was generated using the previously described pNTKV1901-frt-*lox*P vector system (23). Protamine^{Cre}, FLPeR, and ER^{Cre} mice were obtained from the Jackson Laboratory, and CD4^{Cre} mice were obtained from Taconic. Germ line-transmitted mice were crossed with FLPeR mice to delete the *Neo* cassette. The subsequent *WASH*$^{+/flox}$ mice were crossed with Protamine^{Cre} mice to generate *WASH*$^{-/-}$ animals (not viable). *WASH*$^{+/flox}$ mice were backcrossed onto C57/B6 mice (Jackson). Cell-specific *WASH* conditional knockout (cKO) mice were generated by crossing *WASH*$^{+/flox}$ mice with CD4^{Cre} or ER^{Cre} mice to produce *WASH*$^{+/flox}$ Cre^{+} animals. These animals were crossed with *WASH*$^{flox/flox}$ mice. *WASH*$^{+/flox}$ Cre^{+} animals were also crossed with OT-II (Jackson), which have a transgenic TCR that is major histocompatibility complex class II (MHC-II) restricted and responds to the OVA$^{323-339}$ peptide. Cre-positive *WASH*$^{+/+}$ and *WASH*$^{+/flox}$ mice have similar levels of WASH protein, whereas *WASH*$^{flox/flox}$ mice demonstrate a substantial reduction (see Fig. 1A). Unless otherwise indicated, *WASH*$^{+/flox}$ Cre^{+} mice are classified as wild-type (WT) mice and *WASH*$^{flox/flox}$ Cre^{+} mice are classified as cKO or WASHout mice. The data presented are from mice that have been backcrossed onto C57/B6 mice for 6 or 10 generations. Mice were housed in a barrier facility, and all experiments were performed with littermate-matched pairs. All procedures were carried out according to the guidelines from and were approved by the Mayo Clinic Institutional Animal Care and Use Committee.

Allelic germ line transmission was detected with standard PCR methods. The oligonucleotides used included WASH (forward, 5′-CGCATTGATCTTCCTATACGC-3′; reverse, 5′-TGTCAGTCCTATGCTTAGTG-3′), Cre (forward, 5′-ACCAGCCAGCTATCAACTCG-3′; reverse, 5′-TTACATTGGTCCAGCCACC-3′) and, as a control, 16S rRNA, (forward, 5′-CTAGGCCACAGAATTGAAAGATCT-3′; reverse, 5′-GTAGGTGGAAATTCTAGCATCATCC-3′).

Primary murine T cell isolation and activation. Unless otherwise indicated, purified murine CD4^{+} populations were obtained by generating a single-cell suspension using 100-μm-pore-size nylon mesh filters (BD Biosciences) from spleens and lymph nodes, followed by red blood cell lysis via incubation with ACK buffer. The subsequent lymphocyte suspensions were purified with MACS CD4^{+} negative selection beads (Miltenyi Biotec) according to the manufacturer's instructions. Flow cytometry following isolation confirmed the purity of CD4^{+} cells was >90%. For long-term observation of the activation state, equal numbers of purified CD4^{+} T cells were cultured in 24-well plates with plate-bound 2C11 αCD3 (5 μg/ml) and soluble 37.51 αCD28 (1 μg/ml) (Bio-X-Cell).

Thymocyte and splenocyte preparation and flow cytometry analysis. Analysis of thymocyte development and T cell subpopulations were performed as previously described (24). Briefly, thymocyte single-cell suspensions were generated using 100-μm-pore-size nylon mesh filters (BD Biosciences) and surface stained with the following reagents: fluorescein isothiocyanate (FITC)-CD8, TCRβ, TCRγδ, CD3ε, B220, CD19, CD11c, DX5, NK1.1, Ter119, Mac1 (BD Pharmingen), phycoerythrin (PE)-TCRβ, CD8, CD3ε PerCP-CD4, allophycocyanin (APC)-CD8, CD25, and APC–Cy7–c-kit (eBioscience). Splenocyte populations were analyzed by generating a single-cell suspension as described above, followed by red blood cell lysis via incubation with ACK buffer. Cell surface staining was performed with reagents noted above. The data were collected on a FACSCanto II (BD Biosciences) and analyzed with FlowJo (TreeStar, Inc.).

Calcium mobilization. Intracellular Ca^{2+} concentrations were assayed as previously reported (25). Briefly, popliteal, axillary, and cervical lymph nodes (LN) were removed from matched mice, and a single cell suspension was created. LN cells were loaded with 5 μM Indo-1 (Sigma) at 37°C for 30 min in Hanks' balanced salt solution (HBSS) plus 10 mM HEPES. Cells were concurrently labeled with CD3-FITC and CD4-PerCPCy5.5 (eBioscience). The cells were washed and resuspended in HBSS plus 1% bovine serum albumin until analysis. The Indo-1-loaded LN cells were incubated with 2C11(αCD3) monoclonal antibody for 5 min, and an Indo-1 baseline was established. 2C11 was cross-linked with addition of rabbit anti-hamster IgG (MP Biomedicals) to initiate Ca^{2+} mobilization. Control samples were not cross-linked with rabbit anti-hamster IgG. Samples were run on an LSR II flow cytometer (BD Bioscience), and data from CD3^{+} CD4^{+} cells were analyzed with FlowJo (TreeStar).

Intracellular pERK staining. Intracellular pERK levels were assayed as previously reported (26). Briefly, popliteal, axillary, and cervical lymph nodes were removed from matched mice and a single cell suspension was created. Cells were activated by incubation with 2C11 αCD3 (10 μg/ml) and 37.51 αCD28 (10 μg/ml), followed by cross-linking with rabbit anti-hamster IgG (MP Biomedicals). Cells were fixed and permeabilized according to the manufacturer's instructions (eBioscience). Cells were stained with FITC-TCRβ and PerCP-CD4 (eBioscience) and pERK (Cell Signaling Technology), followed by anti-rabbit APC (Jackson). Samples were run on a FACSCanto II flow cytometer (BD Bioscience), and data from TCRβ/CD4^{+} cells were analyzed with FlowJo (TreeStar).

Cell supernatant ELISA. For interleukin-2 (IL-2) secretion, purified CD4^{+} cells were cultured in 96-well plates with the indicated concentrations of plate-bound 2C11 αCD3 and soluble αCD28 (1 μg/ml). After EAE induction, single cell suspensions from draining popliteal LN were created, and 1.5×10^{6} cells/ml were cultured with various concentrations of MOG$^{35-55}$ peptide. At the indicated time points, the supernatants were collected, and the levels of secreted cytokine were determined using enzyme-linked immunosorbent assay (ELISA) kits from eBioscience (IL-2 and gamma interferon [IFN-γ]) and Biolegend (IL-17A). Samples were run in triplicate for each independent experiment.

CFSE proliferation assay. Purified CD4^{+} cells were loaded with 2.5 μM CFSE (carboxyfluorescein diacetate succinimidyl ester; eBioscience) immediately after MACS isolation and were cultured in 96-well plates with 3 μg of plate-bound 2C11 αCD3/ml and 1 μg of αCD28 soluble or αCD28 alone/ml as a control. At 72 h cells were stained for CD4 and run on a FACSCanto II flow cytometer (BD Bioscience), and data from CD4^{+} cells were analyzed with FlowJo (TreeStar). FlowJo's proliferation platform was used to determine proliferation statistics. The division index, which represents the average number of cell divisions per cell, was reported.

Thymidine proliferation assay. After red blood cell lysis, the splenocytes were plated in 96-well plates at 1.5×10^{6} cells/ml, and 2C11 αCD3, OVA$^{323-339}$, or MOG$^{35-55}$ peptide at various concentrations were added. After 48 h, tritiated thymidine was added and, 18 h later, the cells were harvested and the thymidine uptake was measured using a β-scintillation counter (Perkin-Elmer). Where noted, 10 mM methyl pyruvate was added to culture medium prior to plating. The results are presented as the counts per minute (cpm).

Flow cytometry surface/intracellular staining and 6-NBDG uptake. Purified CD4^{+} cells were cultured for various time points with or without plate-bound 2C11 as described above. At the indicated time points, the cells were harvested and counted. Equivalent numbers of cells were stained with 7-aminoactinomycin D (7-AAD) and annexin V-APC (eBioscience) or PE-GLUT1 (R&D Systems), APC-Cy7-TCRβ (eBioscience), PE-Cy7-CD28 (eBioscience), FITC–MHC-I (eBioscience), APC-CD44 (BD Bioscience), Pacific Blue-Thy1.2 (eBioscience), PerCP-Cy5.5-CD62L (eBioscience), PE-TfnR (BD Bioscience), APC-CD25 (eBioscience), PE-Cy7-IL7R (eBioscience), PE-Cy7-CD29 (Biolegend), FITC-CD49d (eBioscience), PE-CD18 (Biolegend), PerCPCy5.5-β7 integrin (Biolegend), Pacific Blue-CD11a (eBioscience), and PerCPCy5.5-FoxP3 (eBioscience).

Intracellular staining was performed using fixation and permeabilization buffers from eBioscience. Alternatively, the cells were resuspended in prewarmed medium and incubated with either dimethyl sulfoxide or a 30 μM concentration of the glucose analog 6-[*N*-(7-nitrobenz-2-oxa-1,3-diazol-4-yl) amino]-2-deoxy-D-glucose (6-NBDG; Invitrogen) for 10 min, washed, and stained with 7-ADD. The cells were run on a FACSCanto II flow cytometer (BD Bioscience), and the data were analyzed using FlowJo (TreeStar). The mean fluorescence intensity (MFI) was defined as the geometric mean of the given fluorescent probe. Either 7-AAD or DAPI (4′,6′-diamidino-2-phenylindole) was used in flow cytometry-based experiments to ensure that only live cells were analyzed.

L-Lactate production. Purified $CD4^+$ cells were cultured with or without plate-bound 2C11 and soluble αCD28 for 48 h as described above. The cells were counted after stimulation, and 10^6 cells were replated for 12 h. Supernatants were then collected and assayed for levels of L-lactate according to the manufacturer's instructions with a kit obtained from Eton Bioscience (Research Triangle Park, NC).

Experimental autoimmune encephalitis model. Mice were immunized with 100 μg of 35- to 55-amino-acid MOG peptide emulsified in complete Freund's adjuvant via subcutaneous injection. At the time of MOG immunization and on day 2, mice were injected intraperitoneally with 400 ng of pertussis toxin. Mice were evaluated daily for weight loss and scored based on EAE development. Clinical scores of 1 to 5 were assigned as previously reported (27). Five $CD4^{Cre}$ WT mice and five cKO mice were injected together and scored concurrently for each experimental set.

Immunofluorescence and quantitation. Purified $CD4^+$ cells were cultured for 24 h as described above. Cells were resuspended in prewarmed serum-free medium and allowed to adhere to poly-L-lysine-coated coverslips at 37°C and then immediately fixed with 4% paraformaldehyde. The coverslips were subsequently prepared as previously described (15). Images were obtained with an LSM-710 laser scanning confocal microscope with a 100×/1.4 Oil Plan-Apochromat objective lens using Zen software (Carl Zeiss). Image slices were taken at a depth of 0.33 μm. Figures and overlays were compiled using Adobe Photoshop and Illustrator. In some cases, the gain of the 488-nm laser was decreased when imaging cKO cells compared to WT cells in order to prevent oversaturation when visualizing the localization of GLUT1 and associated molecules due to highly compact areas of staining. Primary antibodies for staining include: rabbit anti-EEA1 (Cell Signaling Technology), rat anti-LAMP1 (BD Bioscience), mouse anti-GLUT1 (AbCam), and hamster anti-TCRα/β (Thermo Scientific). Anti-VPS35 and anti-mWASH antibodies were generated by immunizing rabbits with glutathione *S*-transferase fusion proteins containing amino acid 461 to end of hVPS35 or amino acid 317 to end of mWASH, respectively (Cocalico Biologicals). Conjugated secondary antibodies were purchased from Invitrogen. Cell boundaries were determined by staining F-actin with Alexa Fluor 647-phalloidin (Invitrogen). Colocalization coefficients were determined from a minimum of 30 cells using Zen 2011 software (Carl Zeiss). Punctum counts were determined using ImageJ (National Institutes of Health). Briefly, the red and green channels were split, and each channel was converted into an 8-bit TIFF file and converted into binary format using ImageJ's binary convert function. The number of positively staining puncta were then calculated using ImageJ's particle count function. The minimum punctum size was set to 50 pixels. Fifty cells from two independent experiments were analyzed, for a total of 100 cells.

Cell stimulation, immunoblotting, and bafilomycin A1 treatment. For short-term TCR stimulation, purified $CD4^{Cre}$ WASHout $CD4^+$ cells were incubated with 2C11 αCD3 (10 μg/ml) and 37.51 αCD28 (10 μg/ml) (Bio-X-Cel), followed by cross-linking at 37°C with 20 μg of rabbit anti-hamster IgG (MP Biomedicals)/ml. For IL-2 stimulation, purified ER^{Cre} WASHout $CD4^+$ cells were activated with 2C11/αCD28 for 48 h as described above. Subsequently, cells were cultured for 48 h in 25 U of IL-2/ml to drive proliferation and in 0.5 μM 4-hydroxy tamoxifen (4-OHT) to induce excision of the *WASH* allele. The cells were IL-2 starved for 12 h and then restimulated with 100 U of IL-2/ml. Stimulations were stopped with ice-cold phosphate-buffered saline (PBS), and the cells were lysed with radioimmunoprecipitation assay (RIPA) buffer and immunoblotted according to standard protocols. 4G10 (Upstate/Millipore), pAKT-S473, total AKT, pSTAT5-Y694, and total STAT5 (Cell Signaling Technology), CAPZα and TCRβ G-11/H-197 (Santa Cruz), TCRα H28 hybridoma (kindly provided by Adam Schrum, Mayo Clinic), CD11a/αL integrin (Santa Cruz), CD29/β1 integrin (BD Bioscience), and Glut1 (AbCam) antibodies were used for immunoblotting. Anti-PLCγ1, anti-CCDC53, antistrumpellin, and anti-SWIP have been previously described (16, 28). Jurkat T cells were electroporated as previously reported (15, 29). $CD4^{Cre}$ WASHout $CD4^+$ cells were stimulated as described above and then treated with 150 nM bafilomycin A1 for 12 h prior to cell lysis.

Quantitative RT-PCR. Primary mouse $CD4^+$ T cells were isolated and stimulated as previously described. At each time point, according to the manufacturer's instructions, RNA was isolated from 3×10^6 T cells using an RNeasy minikit (Qiagen). cDNA was transcribed from 0.5 μg of total RNA using a Superscript III reverse transcription-PCR (RT-PCR) kit (Invitrogen) according to the manufacturer's instructions. Amplification and detection of cDNA was performed using SYBR green PCR master mix (Invitrogen) and an ABI Prism 7900HT real-time PCR system (Applied Biosystems). Primers were obtained from Integrated DNA Technologies (Coralville, IA): murine GLUT1(forward, 5′-ACTGTGGTGTCGCTGTTTG-3′; reverse, 5′-CACGATGCTCAGATAGGACATC-3′) and murine RPLP0 (forward, 5′-AGATCCGCATGTCCCTTC-3′; reverse, 5′-CCTTGCGCATCATGGTGTT-3′). Experiments were performed in triplicate using cDNA from three littermate-matched pairs. The fold change of GLUT1 was calculated by standardization to RPLP0 and analyzed according to the $2^{-\Delta\Delta CT}$ method (30).

Statistical analysis. GraphPad Prism (La Jolla, CA) was used to analyze data sets. Unless otherwise indicated, statistics are presented as means ± the standard errors of the mean (SEM) of three or more independent experiments. Significance between data sets was determined using paired two-tailed Student *t* test. *P* values of <0.05 were considered significant.

RESULTS

$CD4^{Cre}$ WASHout mice demonstrate normal T cell development and maturation. Although studies in cell lines indicate that WASH participates in trafficking of receptors from endomembranes, the physiologic function of WASH is unclear. Thus, we generated WASH conditional knockout mice (23) in order to determine the role of WASH in thymocyte development and peripheral T cell function. We found that total WASH knockout results in embryonic lethality around day E7.5 (T. S. Gomez and D. D. Billadeau, data not shown), which is consistent with studies in *Drosophila*, which have shown that WASH is expressed throughout embryogenesis and that *WASH* KO *Drosophila* are not viable (13, 31). Therefore, we crossed $WASH^{flox/+}$ mice with $CD4^{Cre}$ mice to generate $CD4^{Cre}$ $WASH^{flox/flox}$ conditional knockout (WASHout) mice, which allows for specific Cre-mediated excision of *WASH* in T cells in late thymic development (32). We observed by immunoblot that compared to $CD4^{Cre}$ WT controls WASHout mice exhibited barely detectable levels of WASH in mature $CD4^+$ cells isolated from the spleen (Fig. 1A). Interestingly, while peripheral $CD4^+$ cells from WASHout mice exhibited substantially reduced WASH protein levels, WASHout thymocytes only showed a mild reduction in protein levels, indicating that the existing pool of WASH protein following allele excision was likely stable over an extended period of time (Fig. 1B). WASH exists in a large macromolecular complex known as the SHRC, which demonstrates interdependency for complex stability (14–16). As expected, WASH deletion resulted in a concomitant loss of the SHRC components CCDC53, SWIP, and strumpellin in $CD4^+$

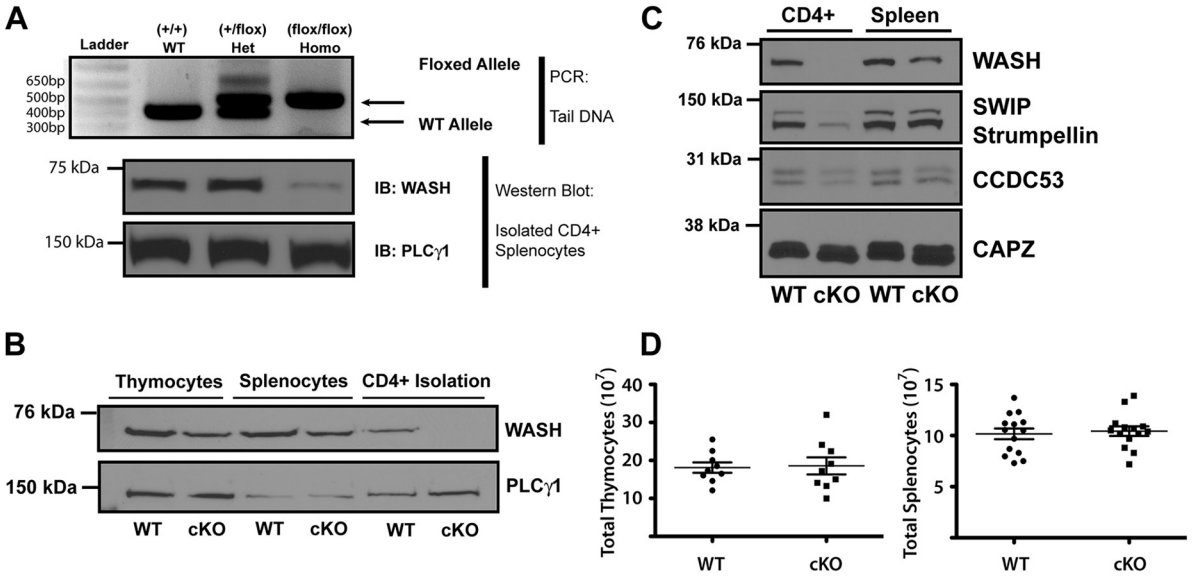

FIG 1 $CD4^{Cre}$ WASHout mice efficiently excise WASH in peripheral T cells and exhibit normal thymic and splenic cellularity. (A) Genotyping oligonucleotides surrounding *wash* exon 2 were utilized to identify WT and floxed *wash* alleles via PCR (top panel), which resulted in either maintenance or loss of WASH protein in isolated splenic $CD4^+$ T cells, as determined by immunoblotting (bottom panel). (B) Total thymocytes, total splenocytes, and isolated splenic $CD4^+$ T cells from $CD4^{Cre}$ WASHout mice and WT littermate-matched controls were lysed. Lysates were resolved by SDS-PAGE and immunoblotted as indicated. (C) Total splenocytes and isolated $CD4^+$ T cells from $CD4^{Cre}$ WASHout and WT mice were collected and lysed. Lysates were resolved by SDS-PAGE and immunoblotted as indicated. (D) $CD4^{Cre}$ WT and WASHout littermate-matched pairs were sacrificed, and the total cellularity of the thymus and spleen following RBC lysis was recorded. Nine pairs are independently plotted, and the means ± the standard error of the mean (SEM) are represented by the bar and whisker overlays.

cells (Fig. 1C). Lastly, we analyzed total thymic and splenic cellularity in WASHout mice and observed no difference compared to $CD4^{Cre}$ WT controls (Fig. 1E). This indicated an absence of gross defects in T cell development or maturation in WASHout mice.

Although normal thymic and splenic cellularity in $CD4^{Cre}$ WASHout mice suggests that thymocyte development proceeds normally in this model, to directly confirm this, we specifically examined the stages of thymocyte development in these mice. As can be seen in Fig. 2A, there was no discernible difference in the percentage of thymocytes found in each stage of T cell development. These percentages were quantified across multiple littermate-matched pairs (Fig. 2B). In addition, we investigated the percentages and subtypes of splenic T cells in WASHout mice. The equivalent splenic cellularity (Fig. 1E) and the percentage of T cells present compared to WT littermate-matched pairs indicated that even in the absence of WASH the peripheral T cell compartments of these WASHout mice were populated normally (Fig. 2C and D). These data indicate that T cells from $CD4^{Cre}$ WASHout mice develop normally and are able to maintain peripheral T cell populations.

Naive WASHout T cells do not demonstrate TCR signaling defects. Our previous work in Jurkat T cells demonstrated that WASH localized to the immune synapse in punctate structures associated with the $EEA1^+$ early endosome compartment (15). Since the endomembrane network has been implicated in receptor trafficking and TCR-stimulated signaling, we isolated $CD4^+$ cells from littermate-matched WT and WASHout mice and examined TCR and CD28 surface levels and T cell activation. Importantly, upon isolation, the levels of TCR and CD28 were similar between WASHout and WT T cells (see Fig. 5A). We next investigated the role of WASH in proximal signaling dynamics by ligating CD3/CD28 *in vitro* and immunoblotting cell lysates for induced protein tyrosine phosphorylation (4G10). Surprisingly, we discovered no defect in global protein tyrosine phosphorylation in WASHout $CD4^+$ T cells following CD3/CD28 ligation, indicating that proximal TCR signaling was intact in WASHout T cells (Fig. 3A). Consistent with this initial observation, no differences in Ca^{2+} mobilization (Fig. 3B) or ERK-phosphorylation (pERK) kinetics (Fig. 3C) were found after activation of naive WT and WASHout T cells. Moreover, surface expression of the activation markers CD69 and CD25 (the high-affinity IL-2 receptor α chain), which are both upregulated after T cell activation, were similar in WT and WASHout T cells after activation (Fig. 3D). Taken together, these data indicate that deletion of WASH does not affect TCR or CD28 cell surface levels on naive T cells or their ability to signal and upregulate activation markers after stimulation.

Naive WASHout T cells produce IL-2 and IL-2 signaling is intact in WASHout T cells. IL-2 is secreted by activated $CD4^+$ T cells and is a critical progrowth cytokine for T cells (33). Thus, although TCR signaling dynamics appeared unaffected, we wanted to further assess the role of WASH in IL-2 production and signaling. We initially investigated IL-2 secretion over time in WT and WASHout T cells by ELISA. Consistent with intact signaling and activation in WASHout T cells, we observed no statistical difference in the amount of IL-2 secreted at 24, 48, or 72 h of stimulation (Fig. 3E). We next investigated the ability of WASHout T cells to efficiently respond to IL-2, which is crucial for T cell expansion. We utilized an inducible WASH cKO system by crossing $WASH^{flox/+}$ mice with ER^{Cre} mice to produce ERC^{Cre} $WASH^{flox/flox}$ (ER^{Cre} WASHout) mice (34). The ER^{Cre} model was used to obtain sufficient numbers of activated WASHout $CD4^+$ T cells (Fig. 3F). After activated $CD4^+$ cells were cultured with 4-OHT for 48 h, WASH protein levels were barely detectable in ER^{Cre} WASHout cells (Fig. 3G). Activated WASHout $CD4^+$ cells were IL-2 starved for 12 h, followed by IL-2 treatment, and IL-2

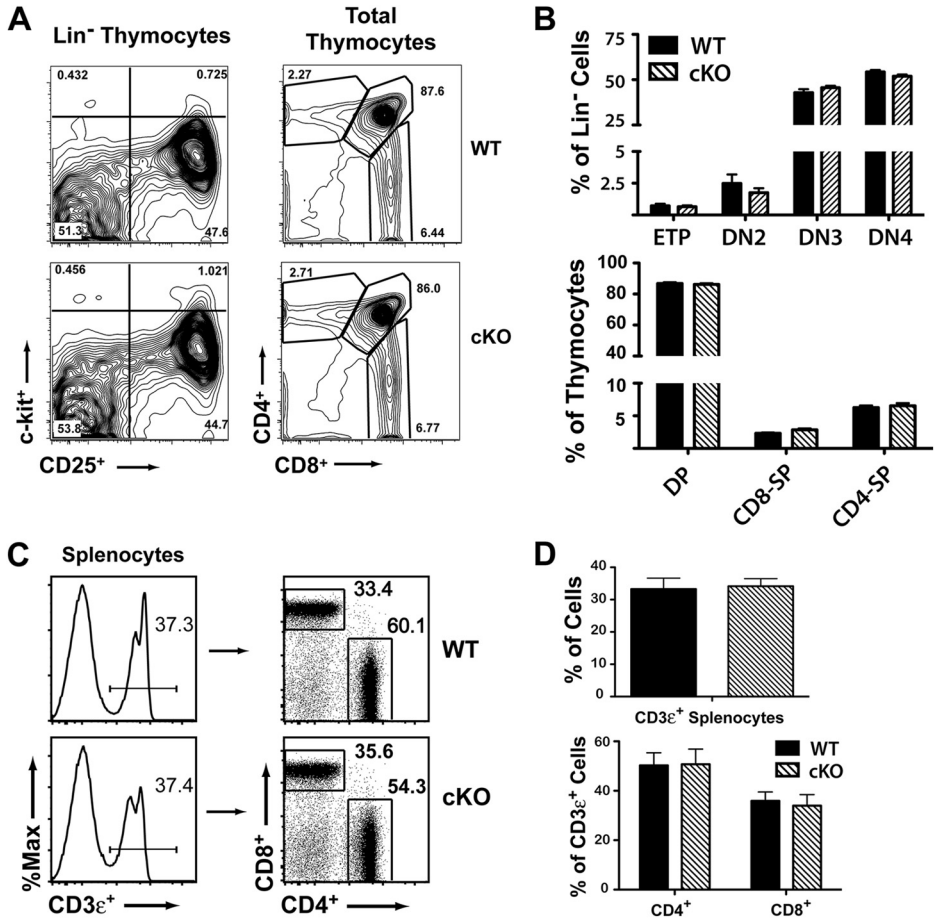

FIG 2 CD4^{Cre} WASHout mice demonstrate normal T cell development and maturation. (A) Representative flow cytometry plots for staining of thymocytes from CD4^{Cre} WT and WASHout mice. Cells were stained and gated as indicated. (B) Top panel shows the percentage of lineage-negative thymocytes in the first four stages (ETP, c-kit$^+$ CD25$^-$; DN2, c-kit$^+$ CD25$^+$; DN3, c-kit$^-$ CD25$^+$; DN4, c-kit$^-$ CD25$^-$) of T cell development, and the bottom panel shows the percentage of thymocytes in the final two stages (double positive and single positive) of development. Values represent the means ± the SEM from five independent CD4^{Cre} littermate matched pairs. (C) Splenocytes from CD4^{Cre} WASHout mice were analyzed by flow cytometry following RBC lysis. The cells were stained and gated as indicated. (D) Percentage of splenic T cells. The upper panel indicates the percentage of CD3ε$^+$ splenocytes, and the lower panel indicates the percentage of CD4$^+$ and CD8$^+$ splenocytes from the CD3ε$^+$ population. Values represent the means ± the SEM from five independent CD4^{Cre} littermate-matched pairs.

signaling was examined by immunoblotting. Importantly, we did not detect a difference in pSTAT5 or pAKT kinetics after IL-2 treatment, indicating that in the absence of WASH, IL-2 signaling was intact (Fig. 3H). Taken together, these data indicate that WASHout CD4$^+$ T cells can secrete and respond to the progrowth cytokine IL-2.

WASHout T cells do not proliferate effectively upon activation. Since the rapid growth and proliferation of activated T cells is an important feature of an intact immune response, we investigated the ability of WASHout CD4$^+$ T cells to proliferate in response to CD3/CD28 ligation. WT and WASHout CD4$^+$ T cells were loaded with CFSE, stimulated for 72 h, and analyzed by flow cytometry to assess the rate of proliferation by CFSE dye dilution. Since loss of WASH did not affect TCR or IL-2 signaling, we were surprised to observe a significant defect in the proliferation of WASHout T cells (Fig. 4A). In fact, the division index for WT T cells was 1.74 ± 0.15, while for WASHout T cells it was less than half that at 0.72 ± 0.15 (Fig. 4B). In addition, we took WT and WASHout splenocytes and stimulated the T cells with increasing concentrations of αCD3ε (2C11) antibody for 48 h and then measured cell proliferation by thymidine incorporation. Similar to the CFSE dilution assay, we observed a significant proliferation defect in the WASHout T cells (Fig. 4C). To confirm that the proliferation defect was not limited to antibody-driven activation of T cells, we utilized CD4^{Cre} WASHout mice crossed to OT-II TCR transgenic mice that are engineered to respond exclusively to MHC-II loaded with the OVA$^{323-339}$ peptide. Consistent with our previous data, CD4^{cre} WT OT-II and WASHout OT-II splenocytes expressed equivalent levels of TCR and CD28 at isolation (data not shown). These cells were stimulated with increasing concentrations of OVA$^{323-339}$ peptide for 48 h and then treated with [^{3}H]thymidine. Significantly, WASHout T cells showed a substantial defect in proliferation over a range of peptide concentrations (Fig. 4D). Since the antigen-presenting cells (splenocytes) in this conditional knockout system are WASH proficient, the inability to proliferate in response to MHC-peptide stimulation is T cell intrinsic. Interestingly, in addition to having a proliferation defect we observed an increased rate of apoptotic cell death in naive WASHout T cells after activation *in vitro* (data available upon request). Since regulatory T cells (Tregs) are known to suppress the immune response (35), we wanted to know whether the pro-

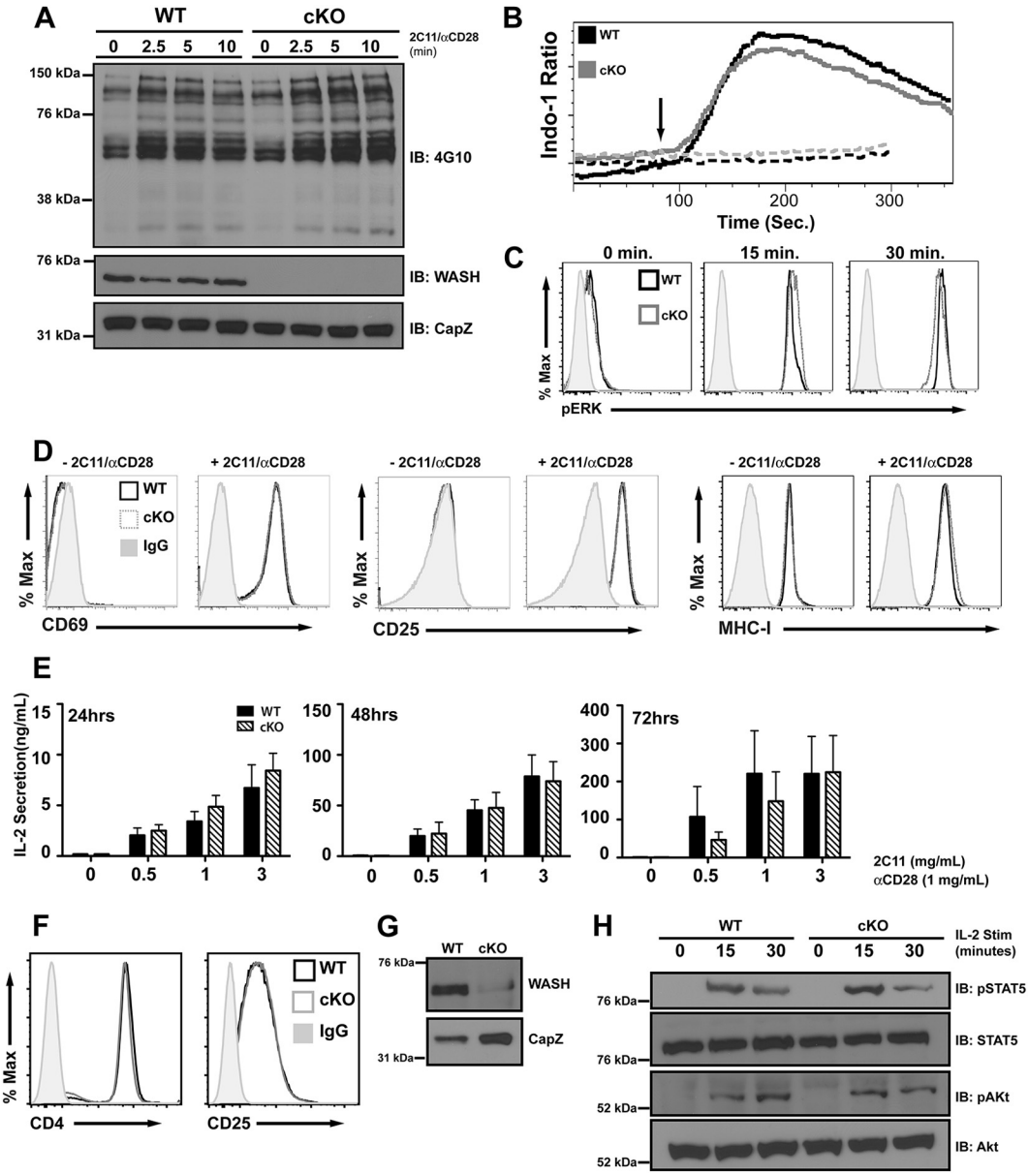

FIG 3 In WASHout T cells TCR signaling and activation are intact. (A) Isolated $CD4^+$ T cells from $CD4^{Cre}$ WASHout and WT mice were activated *in vitro* with 2C11/αCD28 for the indicated times. Ligation was stopped with ice-cold PBS, and the cells were lysed, resolved by SDS-PAGE, and immunoblotted as indicated. The blots are representative of three independent experiments. (B) LN cells of $CD4^{Cre}$ WASHout and WT mice were surface stained for CD3 and CD4 while being loaded with Indo-1. Cells were incubated with 2C11 and activated, and $CD3^+$ $CD4^+$ cells were analyzed by flow cytometry for calcium mobilization. The arrow indicates cross-linking of 2C11 with addition of rabbit anti-hamster IgG. Control cells (dotted line) were not cross-linked. Representative of three independent experiments. (C) LN cells were activated as in panel A and then fixed, permeabilized, and stained with TCRβ, CD4, and pERK. $TCR\beta^+$ $CD4^+$ T cells were analyzed for pERK levels. The results are representative of two independent experiments. (D) Isolated $CD4^+$ T cells from $CD4^{Cre}$ WASHout and WT mice were cultured with plate-bound 2C11 and soluble αCD28 for 24 h and then surface stained with the indicated antibodies and analyzed by flow cytometry. Representative examples shown from four independent experiments. (E) Isolated $CD4^+$ T cells from $CD4^{Cre}$ WASHout and WT mice were plated on 96-well plates coated with the indicated concentrations of 2C11 and soluble αCD28. At the indicated times, IL-2 levels in supernatant were detected by ELISA. Values represent the means ± the SEM from independent $CD4^{Cre}$ littermate-matched pairs. At 24 h, $n = 8$, and at 48 h and 72 h, $n = 4$. (F) Isolated $CD4^+$ T cells from WT and ER^{Cre} WASHout littermate-matched pairs were cultured with plate-bound 2C11 and soluble αCD28 for 48 h and then treated with 4-OHT. After 4-OHT treatment, WASHout T cells had equivalent surface levels of CD25 (IL-2Rα) and (G) reduced WASH protein levels. (H) After 4-OHT treatment, T cells were IL-2 starved and then restimulated with IL-2 for the indicated times. The cells were lysed and immunoblotted as indicated. Representative examples from three independent experiments are shown.

liferation defect was due to increased numbers of Tregs in WASHout mice. However, we did not observe a difference in FoxP3 staining between WT and WASHout T cells (Fig. 4E). In addition, even after 48 h of stimulation, no difference in percentages of $CD4^+$ $Foxp3^+$ cells was observed (Fig. 4F), indicating that the proliferative defect was not the result of Treg suppressor activity. Overall, these data indicate that WASH is required for optimal proliferation of naive T cells after activation.

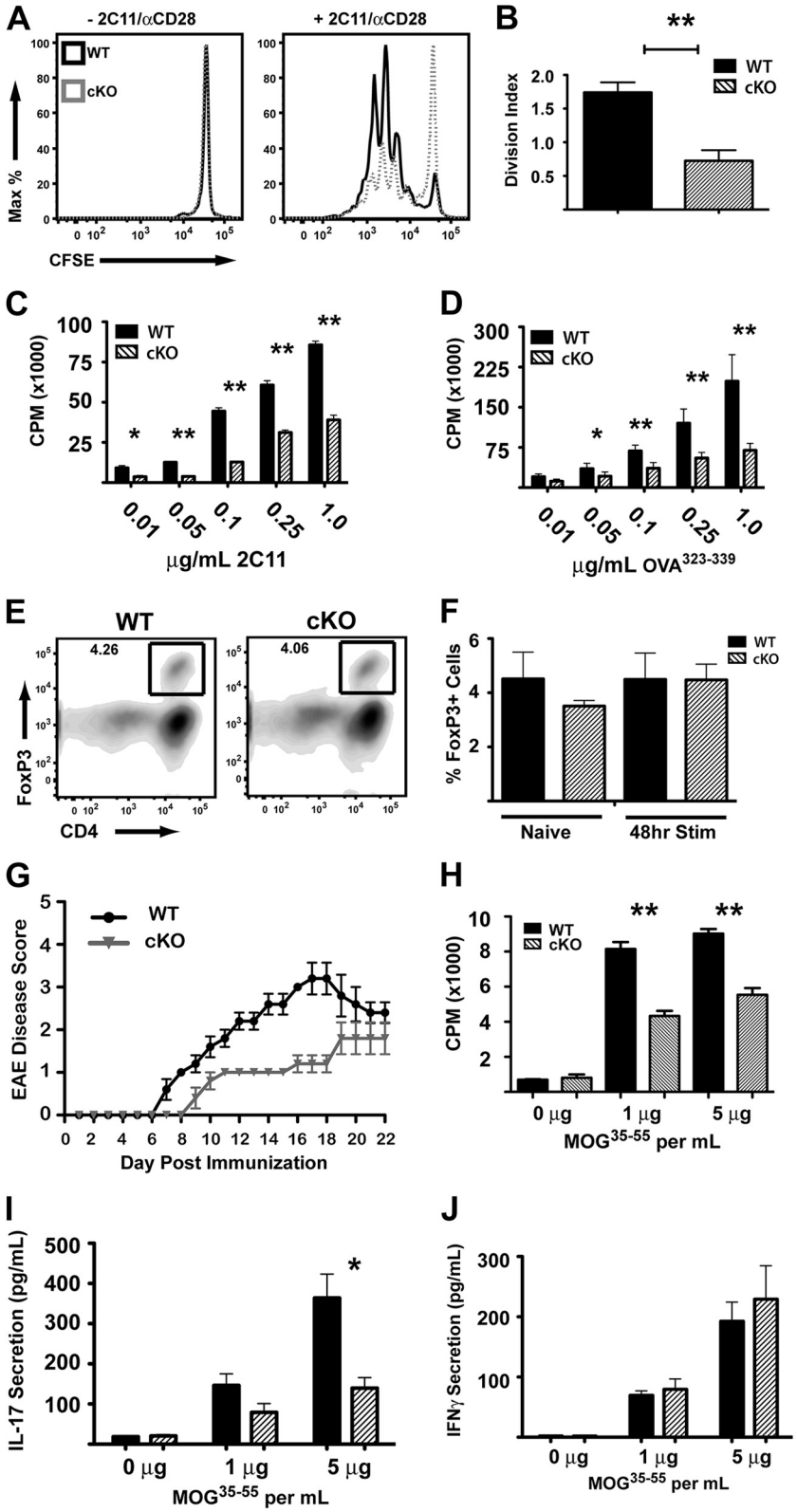

FIG 4 CD4^{Cre} WASHout T cells fail to proliferate following activation and fail to efficiently induce EAE. (A) Isolated CD4^{+} splenocytes were loaded with 5 μM CFSE and stimulated as in Fig. 3E. At 72 h after activation, the cells were analyzed for CFSE dilution. A representative example of seven independent experiments with CD4^{Cre} littermate-matched pairs is shown. (B) Values represent the means ± the SEM of cell division index after 72 h of stimulation and CFSE dilution. The division index was calculated using the proliferation platform in FlowJo. (C and D) After RBC lysis, splenocytes from CD4^{Cre} littermate-matched pairs were stimulated with increasing concentrations of soluble 2C11 (αCD3ε) antibody (C), and CD4^{Cre} OT-II^{+} littermate-matched pairs were stimulated with increasing concentrations of OVA$^{323-339}$ peptide (D). Tritiated thymidine was added after 48 h, the cells were harvested, and the counts per minute (cpm) were analyzed after

EAE is not efficiently induced in CD4^{Cre} WASHout mice. We next wanted to know whether this proliferation defect adversely affected *in vivo* T cell responses. To test this possibility, we utilized experimental autoimmune encephalomyelitis (EAE), a mouse model of T cell-induced autoimmunity. For this model, WASHout and WT mice were immunized with myelin oligodendrocyte glycoprotein amino acid 35 to 55 peptide (MOG$^{35-55}$) and actively monitored for weight loss and clinical signs of disease. WT mice developed ascending limb weakness and paralysis at a greater rate and also exhibited an overall more severe disease phenotype than the WASHout mice (Fig. 4G). Furthermore, 28 days after the initial MOG immunization, cell suspensions from the draining popliteal lymph nodes were restimulated with MOG$^{35-55}$ peptide *in vitro* and proliferation was assessed by thymidine incorporation. Significantly, T cells obtained from the WASHout mice had a substantial decrease in proliferation upon restimulation (Fig. 4H). Since pathogenic effects of EAE can be driven by both Th1 and Th17 T cell subsets, we examined the production of IFN-γ and IL-17 (36). Interestingly, when supernatants from the MOG$^{35-55}$ restimulation cultures were assayed, we observed that WASHout T cells secreted significantly less IL-17, whereas the level of IFN-γ secretion was similar to WT cells (Fig. 4I and J). Taken together, these data indicate that while WASH does not globally regulate TCR signaling or activation-induced IL-2 secretion, WASH does regulate CD4$^+$ T cell proliferation after CD3/CD28 ligation, which results in reduced *in vivo* T cell-mediated immune responses.

Activated WASHout T cells have reduced TCR, CD28, GLUT1, and LFA-1 surface levels. While T cell homeostasis and survival is regulated by multiple signals and pathways (37), our data indicate that WASHout T cells are functionally normal until activated by CD3/CD28 ligation, at which point they fail to proliferate. Since WASH has been implicated in the regulation of receptor trafficking from the endomembranes (14, 15) and in maintaining the structure of the early endosomal and lysosomal compartments (23), we examined the trafficking of specific receptors after T cell activation. Recent work has helped elucidate the underlying mechanisms regulating the endosomal transport and recycling of TCR/CD3 complex after T cell activation (38–40). In addition, the endocytosis and trafficking of the T cell costimulatory receptor CD28 is WASP mediated (41). In light of these reports, we utilized flow cytometry to analyze the surface levels of TCR and CD28 in stimulated cells. To our surprise, WASHout T cells exhibited decreased surface TCR and CD28 after activation, even though the levels of both receptors in naive WASHout T cells were comparable to those in WT T cells (Fig. 5A). Since the TCR is internalized from the cell surface following T cell activation, to ensure that WASHout cells were properly internalizing the TCR and not just delaying internalization, we performed a stimulation time course. We observed that TCR surface levels were equivalently downregulated 12 h after activation, but by 24 h a difference could be observed between WT and WASHout T cells, indicating that the TCR is likely mistrafficked in WASHout T cells following activation (Fig. 5C).

Furthermore, it is well established that quiescent T cells utilize oxidative phosphorylation metabolism as a primary energy source, but switch to aerobic glycolysis when activated (42). This metabolic switch depends on the transcriptional expression and upregulation of the glucose transporter GLUT1 at the cell surface in activated and proliferating T cells (43, 44). Recently, it was shown that proper GLUT1 trafficking was dependent on efficient TCR/CD28 signaling and that restricting glucose uptake in activated T cells resulted in decreased proliferation and survival (45, 46). We therefore examined GLUT1 trafficking after T cell activation in WASHout T cells. Since GLUT1 surface expression is not upregulated until after T cell activation, no difference in GLUT1 surface staining was observed in unstimulated WASHout T cells (Fig. 5A). However, similar to TCR and CD28, following activation, WASHout T cells demonstrated a reduction in surface GLUT1 staining compared to WT controls (Fig. 5A). When the mean fluorescence intensity (MFI) was compared across multiple experiments, the reduction of surface levels of TCR, CD28, and GLUT1 in activated WASHout T cells was found to be statistically significant (Fig. 5B).

Finally, since WASH has been previously reported to regulate α5β1 integrin recycling in human cancer cell lines (19), we examined the fate of integrins in WASHout T cells. Three integrins—LFA-1(αL-β2), VLA-4(α4-β1), and LPAM(α4-β7)—are expressed at low levels on naive T cells and are important for efficient T cell activation and migration (47). We used flow cytometry to determine the surface levels of all alpha and beta subunits in naive WASHout T cells and to our surprise found that only αL (CD11a) was decreased compared to WT (Fig. 5D, upper panel). However, intracellular staining showed that both αL and β2 (CD18), the two components of integrin LFA-1, were decreased in naive WASHout T cells (Fig. 5D, lower panel). When quantitated across multiple experiments, we found a significant difference in the MFIs of these affected integrins (Fig. 5D). Furthermore, we observed the same phenotype of reduced integrin staining in activated WASHout T cells as seen in naive cells (data available upon request). Interestingly, the surface and intracellular levels of integrin α4, β1, and β7 appear to be unaffected in WASHout cells (Fig. 5D). Finally, when total protein levels were assessed by immunoblot, we observed the same pattern in WASHout T cells as seen by flow cytometry. In freshly isolated splenic CD4$^+$ WASHout T cells, TCRβ, and β1 (CD29) protein levels were unaffected, while the αL integrin levels were reduced (Fig. 5E).

We also examined the expression of a number of other cell surface receptors to determine whether the loss of WASH resulted in a global reduction in T cell membrane receptors after activa-

18 h. The values represent the means ± the SEM of three independent experiments. (E) Representative example of surface staining for CD4$^+$ T cells and intracellular staining for the Treg transcription factor FoxP3 in splenocytes from CD4^{Cre} littermate-matched pairs. Isolated CD4$^+$ cells were subsequently stimulated for 48 h, and the staining was repeated. (F) Values represent the percentages of FoxP3$^+$ CD4$^+$ T cells (Tregs). Means ± the SEM of three independent experiments are shown. (G) CD4^{Cre} WT and WASHout mice were immunized subcutaneously with MOG$^{35-55}$ emulsified in CFA and boosted with pertussis toxin to induce experimental autoimmune encephalitis. Weight loss and disease progression were monitored daily. The *y* axis represents the mean clinical scoring from two independent experimental groups ± the SEM. (H) At 28 days after immunization, cells from popliteal lymph nodes were restimulated with the MOG$^{35-55}$ peptide. Tritiated thymidine was added after 48 h, the cells were harvested, and counts per minute (cpm) were analyzed after 18 h. The values represent the means ± the SEM of five independent experiments. Supernatants were collected 48 h after MOG$^{35-55}$ restimulation, and the levels of secreted IL-17A (I) and IFN-γ (J) were determined by ELISA. Values represent the means ± the SEM of five independent experiments. **, $P \leq 0.01$; *, $P \leq 0.05$.

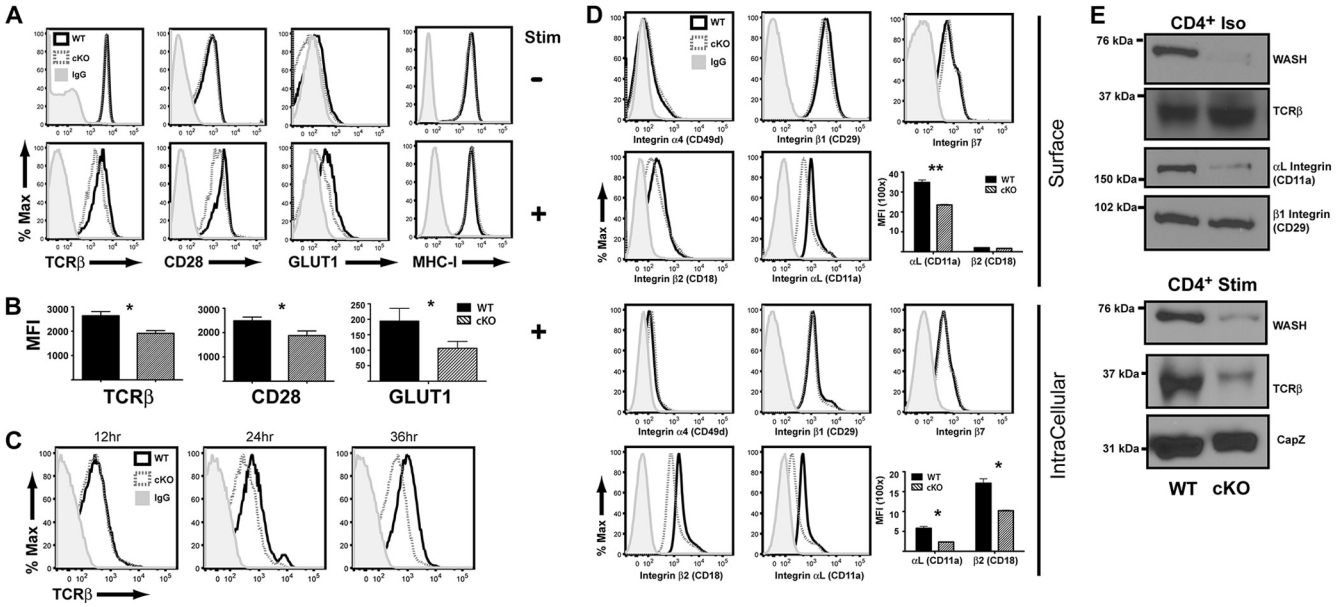

FIG 5 Activated CD4^{Cre} WASHout T cells are unable to maintain surface TCR, CD28, GLUT1, and LFA-1 levels. Isolated CD4$^+$ T cells from CD4^{Cre} WASHout and WT littermate-matched pairs were cultured with or without plate-bound 2C11 and soluble αCD28 for 48 h. (A) Cells were stained for indicated surface markers and analyzed by flow cytometry. (B) MFIs of indicated surface stains after 48 h of T cell activation. Values represent the mean MFI ± the SEM from a minimum of four independent experiments. (C) Isolated T cells were stimulated for 12, 24, and 36 h and then stained for surface levels of TCRβ. Representative plots from three independent experiments are shown. (D) Isolated CD4$^+$ T cells from CD4^{Cre} WASHout and WT littermate-matched pairs were surface stained (top panel) or stained intracellularly (bottom panel) for the indicated integrins. Bar graph values represent the mean MFIs ± the SEM for CD11a and CD18 from three independent experiments. The filled histogram represents IgG control antibody-stained WT cells, the dashed histogram represents WASHout cells, and the black histogram represents WT cells. **, $P \leq 0.01$; *, $P \leq 0.05$. (E) Cells were lysed before (Iso) or after (Stim) stimulation and immunoblotted as indicated. Blots are representative of three independent experiments.

tion. As can be seen in Fig. 5A, the levels of MHC-I were found to be unchanged (Fig. 5A), as were a number of other surface markers (CD44, Thy1.2, CD62L, and IL-7R) in naive and activated WASHout T cells (data available upon request). Taken together, these results suggest that WASH is involved in the selective trafficking of receptors and transporters involved in T cell proliferation and survival.

TCR and GLUT1 localize to collapsed EEA1$^+$ and LAMP1$^+$ compartments in activated WASHout T cells. It was previously shown that TCR surface levels are primarily maintained on T cells by recycling of the TCR complex (48). In addition, it was demonstrated that GLUT1 cell surface expression is maintained in hematopoietic cells by a Rab11a-dependent recycling pathway (49). Since WASH is involved in receptor trafficking (14, 15), we hypothesized that WASH plays a role in TCR and GLUT1 trafficking and that this regulation may provide a mechanism for reduced surface levels of TCR and GLUT1 in activated WASHout T cells. To investigate this possibility, CD4$^+$ T cells from WT and CD4^{Cre} WASHout mice were stimulated with CD3/CD28 ligation for 24 h and confocal microscopy was used to observe the intracellular localization of WASH and TCR. In line with previous observations in Jurkat T cells (15), a punctate pattern of WASH staining was observed in WT T cells and, as expected, was absent from WASHout T cells (Fig. 6A and 7A). Importantly, TCR could be found in puncta that were adjacent to WASH puncta (Fig. 6A), and while GLUT1 demonstrated weak and diffuse membrane staining, it could also be found in puncta adjacent to WASH staining (Fig. 7A). Interestingly, in contrast to WT T cells, TCR and GLUT1 staining in WASHout T cells exhibited a more focused region of intracellular staining (Fig. 6A and 7A).

We have previously shown in WASHout mouse embryonic fibroblasts (MEFs) that the retromer-rich and EEA1$^+$ endosomal compartments collapse in the absence of WASH (23). Thus, we suspected that the localized region of TCR and GLUT1 staining in activated WASHout T cells resulted from endosomal collapse and subsequent receptor accumulation within this compartment. In fact, in contrast to WT T cells, which showed multiple EEA1$^+$ endosomes (Fig. 6B and 7B, upper panel), WASHout T cells had a collapsed EEA1$^+$ endosomal compartment (Fig. 6B and 7B, lower panel). Significantly, while both TCR and GLUT1 were observed in several intracellular puncta juxtaposed to EEA1$^+$ structures in WT T cells, TCR and GLUT1 staining appeared to have increased colocalization with the collapsed EEA1$^+$ stained structures in the WASHout T cells (Fig. 6B and 7B). Interestingly, in naive T cells with visible levels of GLUT1 staining, EEA1 and GLUT1 could still be found together in WT cells, and although the EEA1$^+$ endosomal network appeared collapsed in naive WASHout T cells, the phenotype was not as dramatic as in activated T cells (data not shown).

Since TCR and GLUT1 appeared to undergo aberrant trafficking in activated WASHout T cells, we hypothesized that instead of being recycled to the cell surface in the absence of WASH, TCR, and GLUT1 were trafficked to the lysosome leading to degradation. To investigate this possibility, we stained activated T cells for TCR and GLUT1, along with the lysosomal marker LAMP1. Interestingly, although we observed a limited amount of TCR and GLUT1 colocalization with LAMP1 in WT cells (Fig. 6C and 7C, upper panel), in WASHout T cells we found an increased incidence of TCR and GLUT1 colocalization with LAMP1 (Fig. 6C and 7C, lower panel; the quantification is shown in Fig. 6D and

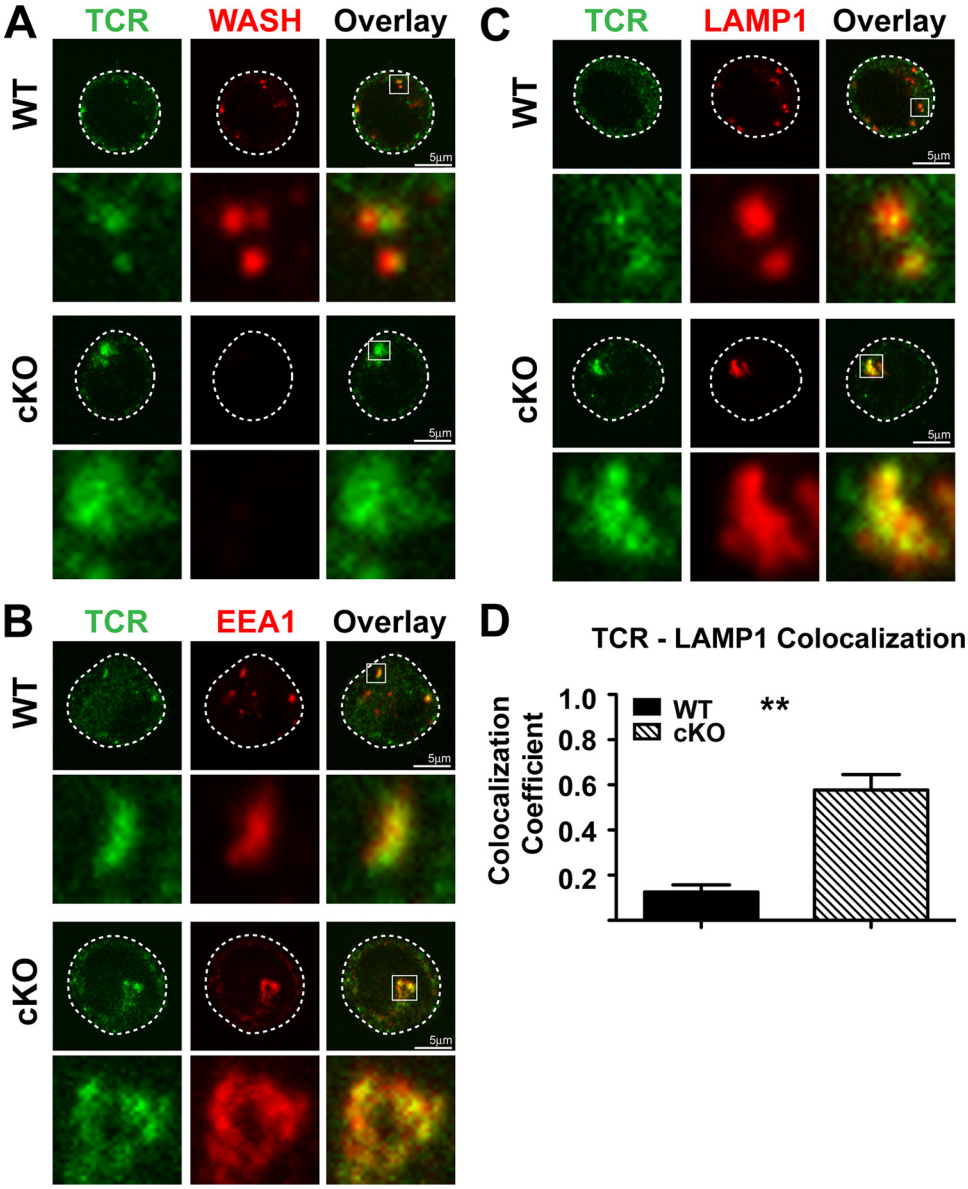

FIG 6 TCR localizes to collapsed EEA1$^+$ and LAMP1$^+$ compartments in activated WASHout T cells. (A to C) Isolated CD4$^+$ T cells from CD4^{Cre} WASHout and WT mice were cultured with plate-bound 2C11 and soluble αCD28 for 24 h. The cells were placed on poly-L-lysine-coated coverslips and stained with primary antibodies against WASH (red) and TCR (green) (A), EEA1 (red) and TCR (green) (B), and LAMP1 (red) and TCR (green) (C), followed by incubation with appropriate secondary antibodies. Cells were imaged with a confocal microscope. White boxes indicate areas of increased magnification that are displayed underneath. Panels are representative examples from two independent experiments. The dotted line represents the plasma membrane boundary. Scale bar, 5 μm. (D) Values represent the colocalization coefficient ± the SEM of TCR with LAMP1 from 30 cells. **, $P \leq 0.01$.

7D). Importantly, LAMP1 staining in cKO WASH T cells indicated a collapsed lysosomal compartment similar to the previously observed pattern of EEA1 staining. This phenotype of lysosomal collapse has also been observed in WASHout MEFs (23). As can be seen, WT T cells have a relatively even distribution of GLUT1 or LAMP1 puncta, whereas WASHout T cells primarily contain only one or two GLUT1 or LAMP1 puncta (Fig. 7D, lower panel). Taken together, these data indicate that in the absence of WASH, intracellular TCR and GLUT1 become trapped in the collapsed endosomal network and instead of being trafficked by the SHRC, they are instead accumulated in the lysosome and likely degraded.

TCR and GLUT1 are degraded in lysosomes in the absence of WASH and retromer. We had already observed that total TCR protein levels are reduced in activated WASHout T cells (Fig. 5E) and, since our data indicate that both TCR and GLUT1 become trapped in the collapsed endosomal network and subsequently accumulate in the LAMP1$^+$ lysosomes, we hypothesized that total GLUT1 protein levels and not just surface levels should also be reduced in activated WASHout T cells due to lysosomal degradation. To test this hypothesis, we isolated peripheral CD4$^+$ T cells and ligated CD3/CD28 for either 24 or 48 h and immunoblotted for total GLUT1 protein levels. Consistent with previous surface staining, we observed a loss of GLUT1 following T cell activation

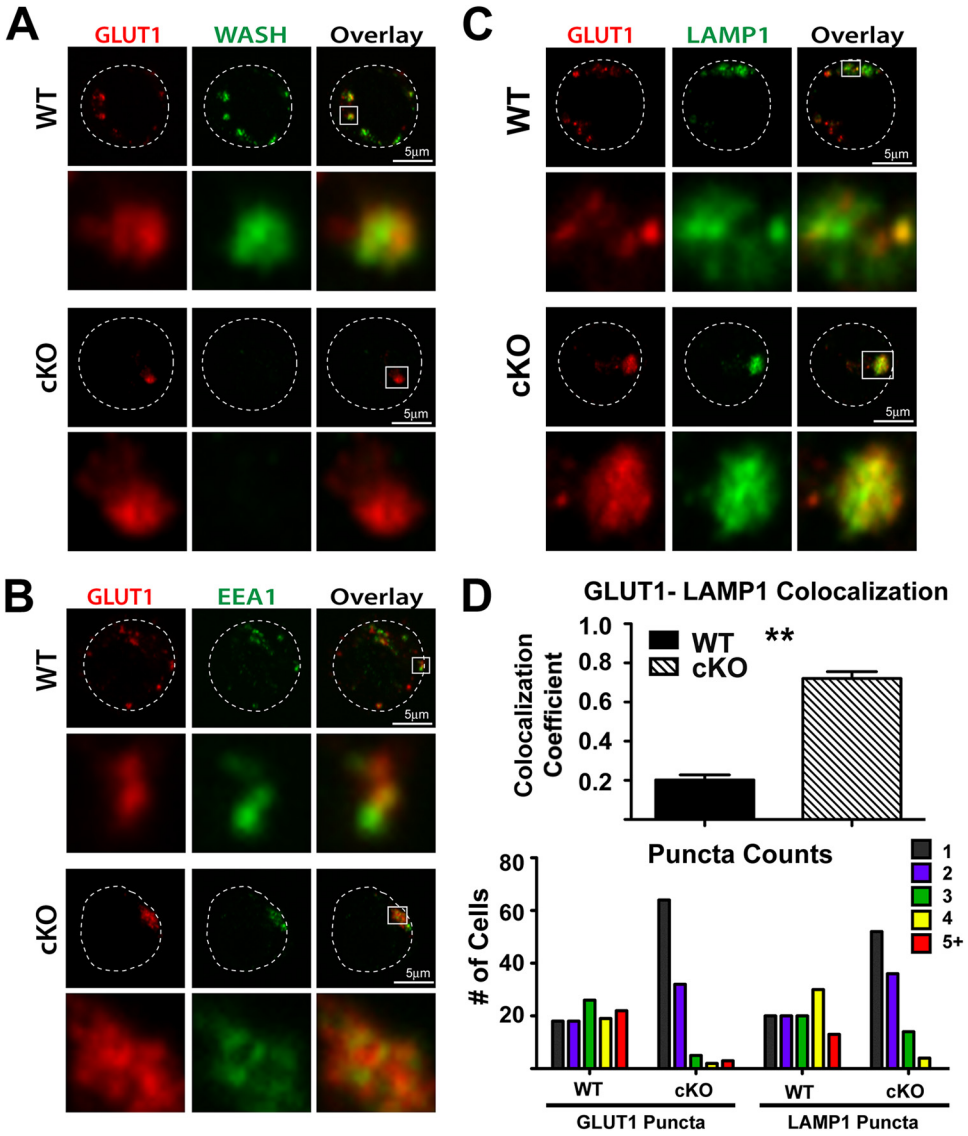

FIG 7 GLUT1 localizes to collapsed EEA1$^+$ and LAMP1$^+$ compartments in activated WASHout T cells. (A to C) Isolated CD4$^+$ T cells from CD4^{Cre} WASHout and WT mice were cultured with plate-bound 2C11 and soluble αCD28 for 24 h. The cells were placed on poly-L-lysine-coated coverslips and stained with primary antibodies against WASH (red) and GLUT1 (green) (A), EEA1 (red) and GLUT1 (green) (B), and LAMP1 (red) and GLUT1 (green) (C), followed by incubation with appropriate secondary antibodies. The cells were imaged with a confocal microscope. White boxes indicate areas of increased magnification that are displayed underneath. The panels show representative examples from three independent experiments. The dotted line represents the plasma membrane boundary. Scale bar, 5 μm. (D) The top panel shows the colocalization coefficient ± the SEM of GLUT1 with LAMP1 from 30 cells. The bottom panel shows the number of distinct LAMP1 and GLUT1 puncta per cell quantitated in activated CD4$^+$ cells. A total of 50 cells from two independent experiments were counted for a total $n = 100$. **, $P \leq 0.01$.

(Fig. 8A). Since the expression of GLUT1 is upregulated after T cell activation, it is possible that reduced GLUT1 gene expression accounts for the reduced protein levels observed in activated WASHout T cells. To test this possibility, we performed RT-PCR to determine the levels of GLUT1 mRNA in WASHout T cells. As expected from our immunoblot results, naive T cells from both WT and WASHout mice have virtually undetectable mRNA levels of GLUT1. Importantly, there was no detectable difference in GLUT1 mRNA expression after CD3/CD28 stimulation, confirming that the observed loss of GLUT1 protein is not due to disrupted gene expression (Fig. 8B). Next, to confirm that in activated WASHout T cells TCR and GLUT1 are degraded in the lysosome, we stimulated CD4$^+$ T cells with CD3/CD28 ligation for 48 h while treating WASHout T cells with the lysosome inhibitor bafilomycin A1 during the final 12 h of stimulation. We observed that WASHout T cells treated with bafilomycin A1 contained significantly increased TCR and GLUT1 protein levels, indicating that in the absence of WASH these proteins are indeed trafficked to, and undergo degradation in, the lysosome (Fig. 8C).

Since WASH was previously reported to interact with the retromer component VPS35 through the WASH complex member FAM21 (17, 18) and involved in regulation of retromer-mediated trafficking (15), we sought to test whether loss of the retromer component VPS35 would also affect TCR and GLUT1 intracellu-

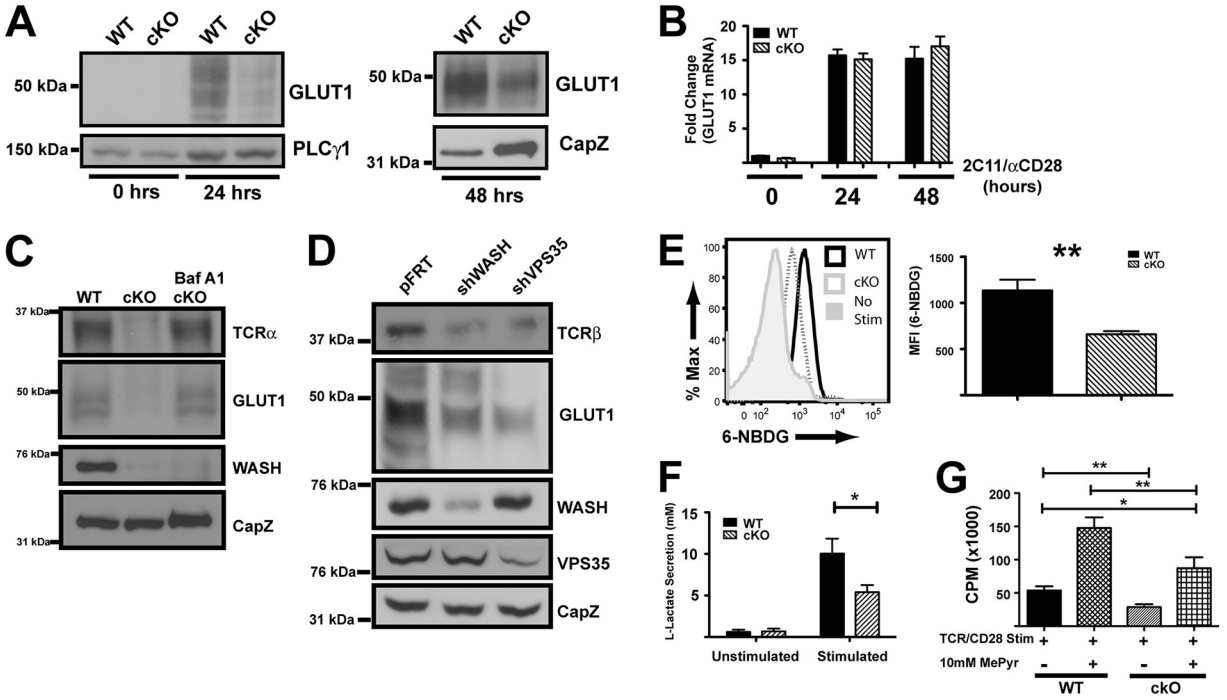

FIG 8 Reduced TCR and GLUT1 levels following activation is due to increased lysosomal degradation resulting in reduced glucose uptake. (A) T cells were lysed before and after stimulation and immunoblotted as indicated. Blots are representative of three independent experiments. (B) mRNA was extracted from T cells before and after stimulation, and RT-PCR was performed. GLUT1 signal was normalized to RPLP0. Values represent the mean fold change from unstimulated WT ± the SEM from a representative experiment performed in triplicate. RT-PCR was performed on three independent littermate-matched pairs. (C) Isolated $CD4^+$ T cells from $CD4^{Cre}$ WASHout and WT mice were stimulated for 48 h. WASHout T cells were treated with or without the lysosome inhibitor bafilomycin A1 for the final 12 h of stimulation. The cells were lysed and immunoblotted as indicated. The blots are representative of two independent experiments. (D) Jurkat T cells were electroporated with shRNA against WASH and VPS35. The cells were cultured for 72 h, lysed, and immunoblotted as indicated. The blots are representative of three independent experiments. (E) After 48 h of activation, primary mouse $CD4^+$ T cells were incubated with the fluorescent glucose analog 6-NBDG, and uptake was assayed by flow cytometry. The filled histogram represents the unstimulated WT 6-NBDG uptake (negative control), the dashed histogram represents the WASHout 6-NBDG uptake, and the black histogram represents WT 6-NBDG uptake. Values in the right panel represent the mean MFIs ± the SEM from five independent experiments. (F) After 48 h of activation, the cells were counted, and 10^6 cells were replated for 12 h. The supernatants were assayed for the presence of L-lactate. Values represent the mean concentrations (mM) ± the SEM from three independent experiments. (G) T cells were stimulated for 48 h with 2C11 and αCD28 with or without 10 mM methyl pyruvate (MePyr). Tritiated thymidine was added, the cells were harvested, and the counts per minute (cpm) were analyzed after 18 h. Values represent the means ± the SEM of five independent experiments. *, $P \leq 0.05$; **, $P \leq 0.01$.

lar trafficking. To do this, we utilized Jurkat T cells, which, like all T cells, endogenously express TCR but also have high constitutive GLUT1 protein levels. Upon shRNA-mediated suppression of WASH or VPS35, there was substantial loss of both total TCR and total GLUT1 protein levels (Fig. 8D). This result prompted us to examine whether GLUT1 might localize with the retromer in primary mouse T cells. Interestingly, when we costained for GLUT1 and VPS35 in activated T cells we observed that some of the intracellular GLUT1 puncta were colocalized with VPS35. Strikingly, in WASHout T cells, we observed a collapsed VPS35 endosomal compartment similar to our EEA1 staining, and GLUT1 and VPS35 exhibited a significant degree of colocalization with VPS35 (data available upon request). Taken together, these data indicate that both WASH and retromer are important for the proper trafficking of TCR and GLUT1 and that in the absence of these regulators TCR and GLUT1 are aberrantly trafficked to the lysosome and degraded.

Activated WASHout T cells experience inefficient glycolysis. Finally, we investigated whether decreased GLUT1 on activated WASHout T cells affected glucose uptake since the primary form of metabolism in activated T cells is aerobic glycolysis (42), which is important for efficient T cell survival and proliferation (43, 44). To examine glucose uptake, we utilized the nonhydrolyzable fluorescent glucose analog 6-[*N*-(7-nitrobenz-2-oxa-1,3-diazol-4-yl) amino]-2-deoxy-D-glucose (6-NBDG). Consistent with reduced GLUT1 surface expression after 48 h of activation, we observed a reduction in 6-NBDG uptake in WASHout T cells compared to WT controls (Fig. 8E). No difference in 6-NBDG uptake was observed in unstimulated T cells (data not shown).

When activated T cells switch their metabolism to aerobic glycolysis the increased rate of glucose catabolism results in pyruvate being converted into lactate instead of acetyl coenzyme A. As a result, we sought to use lactate production by $CD4^{Cre}$ WASHout T cells as an additional readout for glucose uptake and subsequent catabolism. We stimulated purified $CD4^+$ T cells for 48 h and then counted the cells and replated equal numbers of WT and WASHout T cells for 12 h. We then collected supernatants and assayed the media for the presence of L-lactate. As expected, we observed minimal L-lactate secretion in unstimulated T cells and yet, in line with our previous results, we observed a statistically significant decrease in L-lactate secretion from CD3/CD28-stimulated WASHout T cells (Fig. 8F). Since limiting glucose uptake has been shown to reduce primary mouse T cell proliferation capacity (45), we hypothesized that supplementing WASHout T cells with methyl pyruvate (MePyr), a cell-permeable metabolic intermedi-

ate, might rescue the WASHout proliferative defect by satisfying the metabolic demands of T cell activation. Interestingly, as assessed by [^{3}H]thymidine uptake 48 h after activation, TCR/CD28-stimulated WASHout T cells treated with MePyr showed a substantial increase in proliferation compared to either WT or WASHout T cells (Fig. 4G). However, WT T cells treated with MePyr out proliferated WASHout T cells (Fig. 8G). This indicates that while reduced glucose uptake in activated WASHout T cells does limit proliferative capacity it is not the sole mechanism underlying the observed proliferation defect. Taken together, these data indicate that after activation, CD4$^+$ WASHout T cells are unable to maintain GLUT1 surface expression resulting in diminished glucose uptake, leading to a reduced rate of aerobic glycolysis compared to WT T cells and that in the presence of adequate metabolic precursors such as MePyr WASHout cells are able to increase their proliferative capacity.

DISCUSSION

In this report we have provided the initial characterization of a conditional WASH knockout (WASHout) mouse, specifically describing the role of WASH in T cell function. Previous work has shown that WASH regulates trafficking of receptors from endomembranes (14, 15, 50). In fact, WASH has been implicated in the efficient recycling of integrins and epidermal growth factor receptor (14, 19) and shown to play a role in retromer-mediated trafficking (15, 17) and in regulating the recycling of the V-ATPase transporter in *Dictyostelium* (51). Our data suggest that WASH is critical for proper trafficking of the T cell stimulatory receptors TCR and CD28, the integrin LFA-1, and the glucose transporter GLUT1. This report demonstrates the importance of WASH in the regulation of intracellular trafficking of these four receptors/transporter and identifies a physiological proliferation defect in the absence of WASH function. Furthermore, this report provides key insights into the regulation of, and alterations in, endosomal recycling before and after T cell activation.

In the CD4^{Cre} WASHout model we did not observe a defect in thymocyte development. This finding is not surprising given that the CD4^{Cre} system does not induce efficient excision until the DP stage of development (32) and that WASH protein was not totally depleted in thymocytes. However, our data do not preclude the possibility that WASH is involved in thymic development. Previous reports looking at AKT and Notch signaling have hinted at an important role for the maintenance of GLUT1 expression and glucose uptake early in thymocyte development (49, 52, 53), and it has been well established that tightly regulated TCR expression and signaling is required for proper progression at multiple stages in thymocyte development (54). Furthermore, ICAM-1 ligation of LFA-1 on thymocytes has been shown to provide costimulation required for development of single positive thymocytes (55). In light of these past reports and our current findings that WASH is required to maintain TCR, CD28, and LFA-1 surface levels, as well as for efficient GLUT1 trafficking, it will be important to further investigate the role of WASH in thymocyte development by deleting WASH early in thymocyte precursors.

Although we did not observe a defect in thymocyte development in WASHout mice, we also did not observe a difference in peripheral T cell numbers or subpopulations in unchallenged mice. Interestingly, estrogen-related receptor α (ERRα) has been identified as a regulator of metabolic function in T cells (56). Similar to CD4^{Cre} WASHout mice, ERRα$^{-/-}$ mice did not exhibit a defect in T cell homeostasis. However, T cells in aged ERRα$^{-/-}$ mice did not develop an effector/memory phenotype and instead remained in a naive state (56). Although we have not analyzed aged mice in the present study, it would be interesting to examine whether aged WASHout mice exhibit an abnormal immune phenotype. Interestingly, we observed that WASHout T cells exhibit increased rates of apoptotic death after TCR/CD28 activation. Although T cells are known to undergo activation-induced apoptosis (57), it appears that the reduced levels of TCR and CD28 in WASHout T cells do not adversely affect this process. However, increased apoptosis would be consistent with decreased GLUT1 expression in WASHout T cells since disrupted GLUT1 expression and diminished glycolysis results in increased T cell apoptosis (45, 53, 58). Furthermore, WASHout T cells exhibit reduced GLUT1 levels and reduced glucose uptake, which negatively impacts proliferative ability in line with existing reports that glucose restriction reduces T cell proliferation (45).

While in naive T cells the TCR is continuously expressed on the cell surface via internalization and recycling back to the plasma membrane, new reports are helping to elucidate the changes that occur after T cell activation (48). In particular, upon activation, SNARE complexes regulate the polarized recycling of TCR toward the IS (39). Our findings that cell surface TCR levels are normal in naive WASHout T cells but are dramatically reduced after activation suggest that WASH may regulate trafficking pathways that are activated following T cell stimulation to maintain TCR levels. This would be consistent with current indications that multiple transport pathways pass through the endosomal network where differential sorting and trafficking of cargo proteins takes place (59, 60).

Our results demonstrate that CD4^{Cre} WASHout T cells possess normal TCR signaling and that early activation proceeds normally. This is important for proper T cell metabolic function since it is known that both TCR signaling (58) and CD28 costimulation (45, 61) are required for proper GLUT1 upregulation and cell surface localization. Efficient TCR signaling in WASHout T cells is confirmed by the finding that GLUT1 mRNA is equivalently upregulated in following TCR/CD28 stimulation, as are several other activation receptors (e.g., CD69 and CD25). In addition to efficient TCR signaling and activation, WASHout CD4$^+$ T cells produced normal amounts of IL-2, efficiently upregulated the IL-2Rα (CD25), and demonstrated intact IL-2 signaling. This is consistent with the finding that limiting glucose did not affect IL-2 production in T cells (45, 62). As we report, the early endosome network in WASHout cells appears to be collapsed, and this proliferation defect may likely be due to a variety of factors. However, extensive work has documented the delicate nature of properly integrating TCR and CD28 signals in order to achieve a successful T cell response (63, 64). In light of our observed reduction in TCR and CD28 levels after activation, it is possible that whereas initial activation signals appear normal, a lack of sustained TCR/CD28 signaling partially accounts for the reduced proliferation in WASHout T cells. However, more work will be required to confirm this hypothesis. Although recent work has highlighted the importance of sustained and endocytic-based TCR signaling (38, 65), the present study identifies WASH as a key regulator of TCR/CD28 trafficking.

WASH has been previously reported to regulate α5β1 integrin recycling (19); however, we did not observe a defect in either the surface or the total levels of β1 integrin in WASHout T cells. We did, however, find a reduction in intracellular levels of both αL

and β2, which combine to form the integrin LFA-1. Furthermore, we only observed a reduction in surface levels of αL on naive WASHout T cells. Interestingly, internalization and recycling of LFA-1 in T cells has previously been show to be dependent on proper interaction between β2 and Rap-1 (66). In contrast to TCR and GLUT1, which only exhibit surface defects in the activated state, it appears that WASH may regulate LFA-1 trafficking in naive T cells. Recycling of LFA-1 was previously shown to be important for proper cell migration (67), and yet the mechanism behind LFA-1 recycling remains to be clearly elucidated. Although our findings implicate WASH in the regulation of LFA-1 trafficking, further work will be required to determine how and to what extent WASH regulates the cellular localization of both αL and β2 integrins in T cells and how this impacts cell migration and interaction with antigen-presenting cells.

Our data demonstrate that in the absence of WASH, both TCR and GLUT1 are trapped in a collapsed endosomal compartment, resulting in ultimate trafficking to and degradation in the LAMP1$^+$ lysosome. This appears reasonable, since WASH localization at the MVB/lysosomal compartment has been recently reported (14, 19). Also, this finding suggests that WASH is important for proper trafficking of TCR, CD28, LFA-1, and GLUT1, preventing them from entering the lysosome and directing intracellular recycling to the cell surface. Importantly, previous work has demonstrated that the expression of a mutated recycling defect β2 integrin is directed into the late endosome compartment (67). In addition, recent work has proposed differential endosomal trafficking for members of the TCR/CD3 complex (68, 69), and yet the mechanisms behind this trafficking remain unclear. Our data suggest that WASH may be a key regulator of TCR/CD3 complex trafficking in activated T cells and of LFA-1 in either the naive or activated state and that WASH is involved in efficient recycling of these receptors back to the cell surface. Interestingly, both intracellular TCR (39) and GLUT1 (70) have been reported to colocalize with the TfnR, and yet we actually observed an increase in surface TfnR on activated WASHout T cells (data available upon request). In fact, our recent findings in WASHout MEFs (23) confirm these results and further demonstrate that at least in MEFs and T cells, TfnR trafficking is unaltered. Furthermore, our data presented here and in the WASHout MEFs, along with other published reports, indicate that WASH is involved in the trafficking of select membrane receptors. Clearly, there are likely receptors, other than those identified here, that are also trafficked in a WASH-dependent manner that may contribute to the WASHout T cell phenotype of reduced proliferation and EAE induction. Significantly, the WASHout mice generated here will be a useful tool to aid in the identification of receptors and protein complexes that are trafficked in a WASH-dependent manner.

Lastly, it has become clear that the mammalian retromer plays a conserved role in the recycling of certain cargo back to the plasma membrane in collaboration with sorting nexins (71). However, a detailed mechanism of how retromer-mediated recycling functions remains to be elucidated. Significantly, we have previously shown that trafficking of CI-MPR via the mammalian retromer requires WASH-dependent activation of Arp2/3 (15). In this report, we depleted VPS35, a member of the retromer cargo selection complex, in Jurkat T cells and observed the same loss of TCR and GLUT1 proteins, as seen with WASH depletion. Thus, our current results suggest that both WASH and the retromer are required for proper trafficking of TCR and GLUT1 and suggest that the SHRC is a third critical component required for mammalian retromer-mediated receptor trafficking. The cKO WASH mouse model that we describe here will hopefully prove useful in elucidating the physiological function of WASH-dependent trafficking via the retromer in different cell types. In conclusion, we have demonstrated a unique role for WASH in the regulation of T cell proliferation and effector function. This report further supports the importance of proper NPF function in multiple aspects of T cell biology and highlights the role of WASH in efficient trafficking of TCR, CD28, LFA-1, and GLUT1, all of which are critical for effective T cell function.

ACKNOWLEDGMENTS

We thank members of the Billadeau laboratory past and present for helpful discussions and advice. We thank Virginia Shapiro (Mayo Clinic) for reagents, advice on thymocyte development, and critical review of the manuscript. We thank Wojciech Swat (Washington University, St. Louis, MO) for critical review of the manuscript. We also thank Jan van Deursen and the Gene Targeting Core Facility for help with generation of the WASHout mice (Mayo Clinic).

This study was supported by the Mayo Foundation for Medical Research, NIH grant AI065474 to D.D.B. and MSTP grant GM065841 to J.T.P. D.D.B. is a Leukemia and Lymphoma Scholar.

REFERENCES

1. **Lasserre R, Alcover A.** 2010. Cytoskeletal cross-talk in the control of T cell antigen receptor signaling. FEBS Lett. **584**:4845–4850.
2. **Kurisu S, Takenawa T.** 2009. The WASP and WAVE family proteins. Genome Biol. **10**:226.
3. **Rottner K, Hänisch J, Campellone KG.** 2010. WASH, WHAMM, and JMY: regulation of Arp2/3 complex and beyond. Trends Cell Biol. **20**:650–661.
4. **Badour K, Zhang J, Shi F, McGavin MKH, Rampersad V, Hardy LA, Field D, Siminovitch KA.** 2003. The Wiskott-Aldrich syndrome protein acts downstream of CD2 and the CD2AP and PSTPIP1 adaptors to promote formation of the immunological synapse. Immunity **18**:141–154.
5. **Nolz JC, Medeiros RB, Mitchell JS, Zhu P, Freedman BD, Shimizu Y, Billadeau DD.** 2007. WAVE2 regulates high-affinity integrin binding by recruiting vinculin and talin to the immunological synapse. Mol. Cell. Biol. **27**:5986–6000.
6. **Burkhardt JK, Carrizosa E, Shaffer MH.** 2008. The actin cytoskeleton in T cell activation. Annu. Rev. Immunol. **26**:233–259.
7. **Cannon JL, Burkhardt JK.** 2004. Differential roles for Wiskott-Aldrich syndrome protein in immune synapse formation and IL-2 production. J. Immunol. **173**:1658–1662.
8. **Zhang J, Dong B, Siminovitch KA.** 2009. Contributions of Wiskott-Aldrich syndrome family cytoskeletal regulatory adapters to immune regulation. Immunol. Rev. **232**:175–194.
9. **Zipfel PA, Bunnell SC, Witherow DS, Gu JJ, Chislock EM, Ring C, Pendergast AM.** 2006. Role for the Abi/wave protein complex in T cell receptor-mediated proliferation and cytoskeletal remodeling. Curr. Biol. **16**:35–46.
10. **Campellone KG, Webb NJ, Znameroski EA, Welch MD.** 2008. WHAMM is an Arp2/3 complex activator that binds microtubules and functions in ER to Golgi transport. Cell **134**:148–161.
11. **Campellone KG, Welch MD.** 2010. A nucleator arms race: cellular control of actin assembly. Nat. Rev. Mol. Cell. Biol. **11**:237–251.
12. **Zuchero JB, Coutts AS, Quinlan ME, Thangue NBL, Mullins RD.** 2009. p53-cofactor JMY is a multifunctional actin nucleation factor. Nat. Cell Biol. **11**:451–459.
13. **Linardopoulou EV, Parghi SS, Friedman C, Osborn GE, Parkhurst SM, Trask BJ.** 2007. Human subtelomeric WASH genes encode a new subclass of the WASP family. PLoS Genet. **3**:e237. doi:10.1371/journal.pgen.0030237.
14. **Derivery E, Sousa C, Gautier JJ, Lombard B, Loew D, Gautreau A.** 2009. The Arp2/3 activator WASH controls the fission of endosomes through a large multiprotein complex. Dev. Cell **17**:712–723.
15. **Gomez TS, Billadeau DD.** 2009. A FAM21-containing WASH complex regulates retromer-dependent sorting. Dev. Cell **17**:699–711.

16. **Jia D, Gomez TS, Metlagel Z, Umetani J, Otwinowski Z, Rosen MK, Billadeau DD.** 2010. WASH and WAVE actin regulators of the Wiskott-Aldrich syndrome protein (WASP) family are controlled by analogous structurally related complexes. Proc. Natl. Acad. Sci. U. S. A. **107**:10442–10447.
17. **Harbour ME, Breusegem SY, Seaman MNJ.** 2012. Recruitment of the endosomal WASH complex is mediated by the extended "tail" of Fam21 binding to the retromer protein VPS35. Biochem. J. **442**:209–220.
18. **Jia D, Gomez TS, Billadeau DD, Rosen MK.** 2012. Multiple repeat elements within the FAM21 tail link the WASH actin regulatory complex to the retromer. Mol. Biol. Cell **23**:2352–2361.
19. **Zech T, Calaminus SDJ, Caswell P, Spence HJ, Carnell M, Insall RH, Norman J, Machesky LM.** 2011. The Arp2/3 activator WASH regulates α5β1-integrin-mediated invasive migration. J. Cell Sci. **124**:3753–3759.
20. **Temkin P, Lauffer B, SJäger Cimermancic P, Krogan NJ, von Zastrow M.** 2011. SNX27 mediates retromer tubule entry and endosome-to-plasma membrane trafficking of signalling receptors. Nat. Cell Biol. **13**:717–723.
21. **Gomez TS, Billadeau DD.** 2008. T cell activation and the cytoskeleton: you can't have one without the other. Adv. Immunol. **97**:1–64.
22. **Dawlaty MM, van Deursen JM.** 2006. Gene targeting methods for studying nuclear transport factors in mice. Methods **39**:370–378.
23. **Gomez TS, Gorman JA, Artal-Martinez de Narvajas A, Koenig AO, Billadeau DD.** 2012. Trafficking defects in WASH knockout fibroblasts originate from collapsed endosomal and lysosomal networks. Mol. Biol. Cell **23**:3215–3228.
24. **Perchonock CE, Pajerowski AG, Nguyen C, Shapiro MJ, Shapiro VS.** 2007. The related adaptors, adaptor in lymphocytes of unknown function X and Rlk/Itk-binding protein, have nonredundant functions in lymphocytes. J. Immunol. **179**:1768–1775.
25. **Billadeau DD, Mackie SM, Schoon RA, Leibson PJ.** 2000. The Rho family guanine nucleotide exchange factor Vav-2 regulates the development of cell-mediated cytotoxicity. J. Exp. Med. **192**:381–392.
26. **Kortum RL, Sommers CL, Alexander CP, Pinski JM, Li W, Grinberg A, Lee J, Love PE, Samelson LE.** 2011. Targeted Sos1 deletion reveals its critical role in early T-cell development. Proc. Natl. Acad. Sci. U. S. A. **108**:12407–12412.
27. **Mangalam AK, Khare M, Krco C, Rodriguez M, David C.** 2004. Identification of T cell epitopes on human proteolipid protein and induction of experimental autoimmune encephalomyelitis in HLA class II-transgenic mice. Eur. J. Immunol. **34**:280–290.
28. **Ting AT, Karnitz LM, Schoon RA, Abraham RT, Leibson PJ.** 1992. Fc gamma receptor activation induces the tyrosine phosphorylation of both phospholipase C (PLC)-gamma 1 and PLC-gamma 2 in natural killer cells. J. Exp. Med. **176**:1751–1755.
29. **Gomez TS, Hamann MJ, McCarney S, Savoy DN, Lubking CM, Heldebrant MP, Labno CM, McKean DJ, McNiven MA, Burkhardt JK, Billadeau DD.** 2005. Dynamin 2 regulates T cell activation by controlling actin polymerization at the immunological synapse. Nat. Immunol. **6**:261–270.
30. **Livak KJ, Schmittgen TD.** 2001. Analysis of relative gene expression data using real-time quantitative PCR and the $2^{-\Delta\Delta CT}$ method. Methods **25**:402–408.
31. **Rodriguez-Mesa E, Abreu-Blanco MT, Rosales-Nieves AE, Parkhurst SM.** 2012. Developmental expression of *Drosophila* Wiskott-Aldrich syndrome family proteins. Dev. Dyn. **241**:608–626.
32. **Lee PP, Fitzpatrick DR, Beard C, Jessup HK, Lehar S, Makar KW, Pérez-Melgosa M, Sweetser MT, Schlissel MS, Nguyen S, Cherry SR, Tsai JH, Tucker SM, Weaver WM, Kelso A, Jaenisch R, Wilson CB.** 2001. A critical role for Dnmt1 and DNA methylation in T cell development, function, and survival. Immunity **15**:763–774.
33. **Liao W, Lin J-X, Leonard WJ.** 2011. IL-2 family cytokines: new insights into the complex roles of IL-2 as a broad regulator of T helper cell differentiation. Curr. Opin. Immunol. **23**:598–604.
34. **Hayashi S, McMahon AP.** 2002. Efficient recombination in diverse tissues by a tamoxifen-inducible form of Cre: a tool for temporally regulated gene activation/inactivation in the mouse. Dev. Biol. **244**:305–318.
35. **Rudensky AY.** 2011. Regulatory T cells and Foxp3. Immunol. Rev. **241**:260–268.
36. **Jäger A, Dardalhon V, Sobel RA, Bettelli E, Kuchroo VK.** 2009. Th1, Th17, and Th9 effector cells induce experimental autoimmune encephalomyelitis with different pathological phenotypes. J. Immunol. **183**:7169–7177.
37. **Krammer PH, Arnold R, Lavrik IN.** 2007. Life and death in peripheral T cells. Nat. Rev. Immunol. **7**:532–542.
38. **Balagopalan L, Barr VA, Samelson LE.** 2009. Endocytic events in TCR signaling: focus on adapters in microclusters. Immunol. Rev. **232**:84–98.
39. **Das V, Nal B, Dujeancourt A, Thoulouze M-I, Galli T, Roux P, Dautry-Varsat A, Alcover A.** 2004. Activation-induced polarized recycling targets T cell antigen receptors to the immunological synapse; involvement of SNARE complexes. Immunity **20**:577–588.
40. **Finetti F, Paccani SR, Riparbelli MG, Giacomello E, Perinetti G, Pazour GJ, Rosenbaum JL, Baldari CT.** 2009. Intraflagellar transport is required for polarized recycling of the TCR/CD3 complex to the immune synapse. Nat. Cell Biol. **11**:1332–1339.
41. **Badour K, McGavin MKH, Zhang J, Freeman S, Vieira C, Filipp D, Julius M, Mills GB, Siminovitch KA.** 2007. Interaction of the Wiskott-Aldrich syndrome protein with sorting nexin 9 is required for CD28 endocytosis and cosignaling in T cells. Proc. Natl. Acad. Sci. U. S. A. **104**:1593–1598.
42. **Fox CJ, Hammerman PS, Thompson CB.** 2005. Fuel feeds function: energy metabolism and the T-cell response. Nat. Rev. Immunol. **5**:844–852.
43. **Frauwirth KA, Thompson CB.** 2004. Regulation of T lymphocyte metabolism. J. Immunol. **172**:4661–4665.
44. **Michalek RD, Rathmell JC.** 2010. The metabolic life and times of a T-cell. Immunol. Rev. **236**:190–202.
45. **Jacobs SR, Herman CE, MacIver NJ, Wofford JA, Wieman HL, Hammen JJ, Rathmell JC.** 2008. Glucose uptake is limiting in T cell activation and requires CD28-mediated Akt-dependent and independent pathways. J. Immunol. **180**:4476–4486.
46. **MacIver NJ, Jacobs SR, Wieman HL, Wofford JA, Coloff JL, Rathmell JC.** 2008. Glucose metabolism in lymphocytes is a regulated process with significant effects on immune cell function and survival. J. Leukoc. Biol. **84**:949–957.
47. **DeNucci CC, Mitchell JS, Shimizu Y.** 2009. Integrin function in T-cell homing to lymphoid and nonlymphoid sites: getting there and staying there. Crit. Rev. Immunol. **29**:87–109.
48. **Alcover A, Alarcón B.** 2000. Internalization and intracellular fate of TCR-CD3 complexes. Crit. Rev. Immunol. **20**:325–346.
49. **Wieman HL, Wofford JA, Rathmell JC.** 2007. Cytokine stimulation promotes glucose uptake via phosphatidylinositol-3 kinase/Akt regulation of Glut1 activity and trafficking. Mol. Biol. Cell **18**:1437–1446.
50. **Duleh SN, Welch MD.** 2010. WASH and the Arp2/3 complex regulate endosome shape and trafficking. Cytoskeleton **67**:193–206.
51. **Carnell M, Zech T, Calaminus SD, Ura S, Hagedorn M, Johnston SA, May RC, Soldati T, Machesky LM, Insall RH.** 2011. Actin polymerization driven by WASH causes V-ATPase retrieval and vesicle neutralization before exocytosis. J. Cell Biol. **193**:831–839.
52. **Ciofani M, Zúñiga-Pflücker JC.** 2005. Notch promotes survival of pre-T cells at the beta-selection checkpoint by regulating cellular metabolism. Nat. Immunol. **6**:881–888.
53. **Wofford JA, Wieman HL, Jacobs SR, Zhao Y, Rathmell JC.** 2008. IL-7 promotes Glut1 trafficking and glucose uptake via STAT5-mediated activation of Akt to support T-cell survival. Blood **111**:2101–2111.
54. **Hayday AC, Pennington DJ.** 2007. Key factors in the organized chaos of early T cell development. Nat. Immunol. **8**:137–144.
55. **Paessens LC, Singh SK, Fernandes RJ, van Kooyk Y.** 2008. Vascular cell adhesion molecule-1 (VCAM-1) and intercellular adhesion molecule-1 (ICAM-1) provide co-stimulation in positive selection along with survival of selected thymocytes. Mol. Immunol. **45**:42–48.
56. **Michalek RD, Gerriets VA, Nichols AG, Inoue M, Kazmin D, Chang C-Y, Dwyer MA, Nelson ER, Pollizzi KN, Ilkayeva O, Giguere V, Zuercher WJ, Powell JD, Shinohara ML, McDonnell DP, Rathmell JC.** 2011. Estrogen-related receptor-α is a metabolic regulator of effector T-cell activation and differentiation. Proc. Natl. Acad. Sci. U. S. A. **108**:18348–18353.
57. **Zhang J, Cado D, Chen A, Kabra NH, Winoto A.** 1998. Fas-mediated apoptosis and activation-induced T-cell proliferation are defective in mice lacking FADD/Mort1. Nature **392**:296–300.
58. **Rathmell JC, Vander Heiden MG, Harris MH, Frauwirth KA, Thompson CB.** 2000. In the absence of extrinsic signals, nutrient utilization by lymphocytes is insufficient to maintain either cell size or viability. Mol. Cell **6**:683–692.
59. **Cullen PJ.** 2008. Endosomal sorting and signalling: an emerging role for sorting nexins. Nat. Rev. Mol. Cell. Biol. **9**:574–582.

60. **Hsu VW, Prekeris R.** 2010. Transport at the recycling endosome. Curr. Opin. Cell Biol. **22**:528–534.
61. **Frauwirth KA, Riley JL, Harris MH, Parry RV, Rathmell JC, Plas DR, Elstrom RL, June CH, Thompson CB.** 2002. The CD28 signaling pathway regulates glucose metabolism. Immunity **16**:769–777.
62. **Cham CM, Gajewski TF.** 2005. Glucose availability regulates IFN-gamma production and p70S6 kinase activation in $CD8^+$ effector T cells. J. Immunol. **174**:4670–4677.
63. **Gamper CJ, Powell JD.** 2010. Genetic and biochemical regulation of CD4 T cell effector differentiation: insights from examination of T cell clonal anergy. Immunol. Res. **47**:162–171.
64. **Riley JL, Mao M, Kobayashi S, Biery M, Burchard J, Cavet G, Gregson BP, June CH, Linsley PS.** 2002. Modulation of TCR-induced transcriptional profiles by ligation of CD28, ICOS, and CTLA-4 receptors. Proc. Natl. Acad. Sci. U. S. A. **99**:11790–11795.
65. **Cemerski S, Das J, Giurisato E, Markiewicz MA, Allen PM, Chakraborty AK, Shaw AS.** 2008. The balance between T cell receptor signaling and degradation at the center of the immunological synapse is determined by antigen quality. Immunity **29**:414–422.
66. **Tohyama Y, Katagiri K, Pardi R, Lu C, Springer TA, Kinashi T.** 2003. The critical cytoplasmic regions of the αL/β2 integrin in Rap1-induced adhesion and migration. Mol. Biol. Cell **14**:2570–2582.
67. **Fabbri M, Di Meglio S, Gagliani MC, Consonni E, Molteni R, Bender JR, Tacchetti C, Pardi R.** 2005. Dynamic partitioning into lipid rafts controls the endo-exocytic cycle of the αL/β2 integrin, LFA-1, during leukocyte chemotaxis. Mol. Biol. Cell **16**:5793–5803.
68. **Ouchida R, Yamasaki S, Hikida M, Masuda K, Kawamura K, Wada A, Mochizuki S, Tagawa M, Sakamoto A, Hatano M, Tokuhisa T, Koseki H, Saito T, Kurosaki T, Wang J-Y.** 2008. A lysosomal protein negatively regulates surface T cell antigen receptor expression by promoting CD3ζ-chain degradation. Immunity **29**:33–43.
69. **Swamy M, Siegers GM, Fiala GJ, Molnar E, Dopfer EP, Fisch P, Schraven B, Schamel WW.** 2010. Stoichiometry and intracellular fate of TRIM-containing TCR complexes. Cell Commun. Signal **8**:5.
70. **Eyster CA, Higginson JD, Huebner R, Porat-Shliom N, Weigert R, Wu WW, Shen R-F, Donaldson JG.** 2009. Discovery of new cargo proteins that enter cells through clathrin-independent endocytosis. Traffic **10**:590–599.
71. **Cullen PJ, Korswagen HC.** 2012. Sorting nexins provide diversity for retromer-dependent trafficking events. Nat. Cell Biol. **14**:29–37.